
Automatic Policy Synthesis to Improve the Safety of Nonlinear Dynamical Systems

Arash Mehrjou
Max Planck Institute for Intelligent Systems &
ETH Zürich
amehrjou@ethz.ch

Mohammad Ghavamzadeh
Facebook AI Research
mohammad.ghavamzadeh@inria.fr

Bernhard Schölkopf
Max Planck Institute for Intelligent Systems
bs@tuebingen.mpg.de

Abstract

Learning controllers merely based on a performance metric has been proven effective in many physical and non-physical tasks in both control theory and reinforcement learning. However, in practice, the controller must guarantee some notion of safety to ensure that it does not harm either the agent or the environment. Stability is a crucial notion of safety, whose violation can certainly cause unsafe behaviors. Lyapunov functions are effective tools to assess stability in nonlinear dynamical systems. In this paper, we combine an improving Lyapunov function with automatic controller synthesis to obtain control policies with large safe regions. We propose a two-player collaborative algorithm that alternates between estimating a Lyapunov function and deriving a controller that gradually enlarges the stability region of the closed-loop system. We provide theoretical results on the class of systems that can be treated with the proposed algorithm and empirically evaluate the effectiveness of our method using an exemplary dynamical system.

1 Introduction

Nonlinear dynamical systems are the main mathematical tool in studying evolving phenomena in science and engineering. In a categorization, systems can be divided into those on which we can intervene (*non-autonomous*) and those that we cannot intervene on (*autonomous*). Studying the stability region of autonomous systems and designing controllers (Note that we use the terms *policy* and *controller* interchangeably in this work) to drive a non-autonomous system towards a target behavior are of fundamental importance in many disciplines such as aviations [1], haptics [2], autonomous driving [3], and robotics [4]. An indisputable goal for a controller is to stabilize the system. Unlike linear systems, stability is a local property in nonlinear systems. Knowledge of the stability region is essential in many applications such as power system transient stability analysis [5–7], stabilization of nonlinear systems [8–10], design of associative memory in artificial neural networks [11, 12], robotics [13, 14], and biology [15].

Controllers that enhance the stability region of a system, also known as Region of Attraction (RoA), are highly desired as they make more clever use of the inherent nonlinear structure of the system. In almost every application, a feasible controller with a larger RoA is preferred. For example, a fighter aircraft will be able to carry out more aggressive maneuvers and still remain within its safe regime [16]. A power grid system will remain functional under heavier burden [17]. An autonomous driving system will remain safe under more diverse and potentially harsh conditions [18].

A great number of methods for designing a controller [19–22, 20] for nonlinear systems and determining their RoA [23, 24] have been proposed in the literature. Starting with Lyapunov’s thesis [25] at the beginning of 20th century and LaSalle’s extensions [26] followed by a series of results so-called *converse theorems* [27], a concrete study of the stability of dynamical systems has become possible. However, the design of a stabilizing controller has been ad-hoc for every class of nonlinear systems. The idea of *control Lyapunov function (clf)* [28–30] was an effort to unify stability analysis and control synthesis but constructing expression-level (analytical closed-form function) clf and extracting a controller out of it is not straightforward for most nonlinear systems.

Machine learning community has developed a diverse set of tools to work with data when the expression-level analysis is impossible [31, 32]. The recent surge of attention to data-driven control has shown significant success in areas where analytical treatment is inapplicable [33]. Connections between control theory and machine learning have been constructed in various directions. A few of these intersections are touched upon in the following.

Function approximators such as kernel methods [34] and neural networks [35] have been successfully used for system identification. Moreover, ideas from information theory and statistics have been adopted for model selection in system identification [36, 37]. The development of automatic differentiation packages for machine learning has opened up a new approach to stability analysis and estimation of functions of interest in control theory such as Hamiltonian [38] or Lyapunov function [39]. Recent advances in implicit generative models have proven effective in filtering applications where the states of the system are inferred from noisy observations [40]. Nevertheless, The connection between machine learning and control theory is not a one-way path. Many learning algorithms can be simplified to dynamical systems. Especially, the algorithms such as generative adversarial networks [41] and n -player cooperative games have been analyzed as dynamical systems to obtain some insight into the dynamics of learning [42–45] and the emergence of strategies [46, 47]. Control methodologies such as proportional controllers have also been used to address the stability issues of multi-player algorithms such as adversarial networks [48].

In this work, we bring together Lyapunov stability analysis from control theory and function approximators / automatic differentiation from machine learning to build an evolving controller that smoothly enlarges the stability region of the closed-loop system. Our contributions are as follows: **1)** Improving a learning algorithm to estimate the Lyapunov function and RoA, **2)** Combining RoA estimation algorithm with an automatic policy update phase to enlarge the RoA of the system, and **3)** Providing theoretical guarantees for the class of systems in which the training process shows stable behavior. Section 2 goes over the definitions and preliminary materials, Section 3 states the problem that we study in this paper. The proposed algorithm and its theoretical discussion are presented in Section 4. Finally, we empirically evaluate the performance of the proposed method in Section 5, followed by related work and conclusion in Section 6. Most of the proofs, theoretical discussions, and extended experimental results are reported in the appendix.

2 Preliminaries

In this section, we present the definitions and preliminary theoretical results that are required in the rest of this paper.

System— Consider a continuous-time nonlinear disturbance-free dynamical system described by

$$\dot{\mathbf{x}}(t) = f(\mathbf{x}(t), \mathbf{u}(t), t), \quad (1)$$

where $\mathbf{x}(t) \in \mathcal{X} \subseteq \mathbb{R}^d$ and $\mathbf{u}(t) \in \mathcal{U} \subseteq \mathbb{R}^p$ are state and control vectors, and \mathcal{X} and \mathcal{U} are the state and control spaces. We restrict ourselves to the fully observable case, where the states are directly available to a feedback controller, i.e., $\mathbf{u}(t) = \pi(\mathbf{x}(t))$, and π is the feedback law. The function f is the time-independent *dynamics*. Hence, (1) is simplified to $\dot{\mathbf{x}} = f(\mathbf{x}(t))$ that is a time-invariant autonomous (TIA) system. By assuming the Lipschitz continuity of f and π , a unique solution of this system for every initial state exists that is denoted by $\Phi(\mathbf{x}, \cdot) : \mathbb{R} \rightarrow \mathcal{X}$, with $\Phi(\mathbf{x}, 0) = \mathbf{x}$. In practice, it is often easier to discretize the time and work with discrete-time systems defined as

$$\mathbf{x}_{k+1} = f(\mathbf{x}_k, \mathbf{u}_k), \quad (2)$$

where $k \in \mathbb{N}$ is the discrete time index, $\mathbf{x}_k \in \mathcal{X} \subseteq \mathbb{R}^d$ and $\mathbf{u}_k \in \mathcal{U} \subseteq \mathbb{R}^p$ are the state and control signals at time step k .¹ Our algorithm is presented for discrete-time systems but the theoretical discussions are applicable to continuous-time systems as well.

¹As a notational convention, we use subscript for vectors that are sampled at discrete times and arguments for their continuous counterparts, i.e., $\mathbf{x}_k = \mathbf{x}(k\tau)$ where τ is the sampling time interval.

Sets— A state vector $\bar{\mathbf{x}}$ is called an *equilibrium point* of the TIA system f , if $f(\bar{\mathbf{x}}) = \mathbf{0}$. A state vector is called a *regular point* if it is not an *equilibrium point*. Let $J_f(\mathbf{x})$ be the Jacobian of $f(\cdot)$ at \mathbf{x} . If $J_f(\mathbf{x})$ has no eigenvalue with zero real part, \mathbf{x} is called a *hyperbolic equilibrium point*. A hyperbolic equilibrium point is stable if all its eigenvalues have negative real parts; otherwise, it is an *unstable equilibrium point*. A system whose all critical elements (equilibrium points and limit cycles) are hyperbolic is called a hyperbolic system. A set $M \subseteq \mathcal{X}$ is called an *invariant set* if every trajectory of the system starting in M remains in M , for $t \in \mathbb{R}$. A point $\mathbf{p} \in \mathbb{R}^d$ is said to be in the ω -limit set (or α -limit set) of \mathbf{x} if for every $\epsilon > 0$, there exists a $T > 0$, such that $\forall t > T$ ($\forall t < T$), $|\Phi(\mathbf{x}, t) - \mathbf{p}| < \epsilon$. The stable and unstable manifolds of a hyperbolic equilibrium point $\bar{\mathbf{x}}$ are defined as $W^s = \{\mathbf{x} \in \mathcal{X} : \Phi(\mathbf{x}, t) \rightarrow \bar{\mathbf{x}} \text{ as } t \rightarrow \infty\}$ and $W^u = \{\mathbf{x} \in \mathcal{X} : \Phi(\mathbf{x}, t) \rightarrow \bar{\mathbf{x}} \text{ as } t \rightarrow -\infty\}$.

It can be shown that W^s and W^u are both invariant sets [49]. Moreover, $\bar{\mathbf{x}}$ is the ω -limit (α -limit) of every point of its stable (unstable) manifold.

Stability— The point $\bar{\mathbf{x}}$ is said to be a stable equilibrium point, if there exists a $\delta > 0$ such that $\Phi(\mathbf{x}_0, t) \rightarrow \bar{\mathbf{x}}$ as $t \rightarrow \infty$, if $\|\mathbf{x}_0 - \bar{\mathbf{x}}\| < \delta$. If δ can take arbitrarily large values, $\bar{\mathbf{x}}$ is called the *globally stable equilibrium point*. Global stability is rare in natural nonlinear dynamical systems. Nonlinear systems often have a local stability region (RoA) that is defined for the stable equilibrium point $\bar{\mathbf{x}}$ as follows:

$$\mathcal{R}^{\bar{\mathbf{x}}} = \{\mathbf{x} \in \mathcal{X} : \lim_{t \rightarrow \infty} \Phi(\mathbf{x}, t) = \bar{\mathbf{x}}\}. \quad (3)$$

Topologically speaking, $\mathcal{R}^{\bar{\mathbf{x}}}$ is an open, invariant, and connected set. We denote the boundary of this set by $\partial\mathcal{R}^{\bar{\mathbf{x}}}$ that is often topologically a $(n - 1)$ -dimensional closed and invariant set [49, 50].

Functions— The most important sufficient condition for the stability of an autonomous nonlinear system is the existence of a *Lyapunov function (lf)*. As we work with discrete-time dynamics in Section 3, we present the Lyapunov’s stability theorem for discrete-time systems.

Theorem 1 (Lyapunov’s stability theorem [25]). *Let f be a locally Lipschitz continuous dynamics with an equilibrium point at the origin $\bar{\mathbf{x}} = \mathbf{0}$. Suppose there exists a locally Lipschitz continuous function $V = \mathcal{X} \rightarrow \mathbb{R}$ and a domain $\mathcal{D} \subseteq \mathcal{X}$, such that*

$$V(\mathbf{0}) = 0 \quad \text{and} \quad V(\mathbf{x}) > 0 \quad \forall \mathbf{x} \in \mathcal{D} \setminus \{\mathbf{0}\} \quad (4)$$

$$\Delta V(\mathbf{x}) := V(f(\mathbf{x})) - V(\mathbf{x}) < 0 \quad \forall \mathbf{x} \in \mathcal{D} \setminus \{\mathbf{0}\} \quad (5)$$

Then, $\bar{\mathbf{x}}$ is asymptotically stable and V is a Lyapunov function. The domain \mathcal{D} in which Equation (5) is satisfied is called the Lyapunov decrease region.

Corollary 1 (Level sets of a Lyapunov function). *In light of Theorem 1, every level set $\{\mathbf{x} \in \mathcal{X} : V(\mathbf{x}) < c\}$, for $c \in \mathbb{R}_+$, that is contained within \mathcal{D} is invariant under the dynamics of the system.*

3 Problem Statement

Let’s consider a discrete-time TIA system as (2), where the control signal is produced by a feedback-controller $\pi(\cdot; \psi) : \mathcal{X} \rightarrow \mathcal{U}$ parameterized by ψ . Therefore, the closed-loop dynamics denoted by f_π is a functional of the controller and is consequently parameterized by ψ as $\mathbf{x}_{k+1} = f(\mathbf{x}_k, \pi(\mathbf{x}_k; \psi)) = f_\pi(\mathbf{x}_k; \psi)$. Without loss of generality, we assume that the equilibrium point of interest is located at the origin, i.e., $\bar{\mathbf{x}} = \mathbf{0}$. The policy π induces a RoA around the equilibrium point denoted by \mathcal{R}_π .²

Each control task can be broken down into two subtasks: **1)** Controller synthesis and **2)** Closed-loop response evaluation. These steps are dependent as the controller is usually designed to optimize some measure of performance. For example, in optimal control problems, it is intended to find a controller that keeps the states close to a set of target states with minimal control effort. This quantitative measure can be translated to a PDE known as the HJB equation, whose solution is the answer to the optimal control problem [51].

In this work, the performance measure is the size of the stability region. However, despite optimal control problems, this quantity cannot be expressed as a function of the control signal, whose solution gives the maximum stability region. More formally, let $\mu : 2^{\mathcal{X}} \rightarrow \mathbb{R}_+$ be a mapping that assigns to each $A \subseteq \mathcal{X}$ a measure of its size. To prevent pathological cases, we assume \mathcal{X} to be compact with $\mu(\mathcal{X}) < \mu_\infty < \infty$. As a sensible choice, we choose μ to be the Lebesgue measure restricted to $\mathcal{X} \subseteq \mathbb{R}^d$ in the measure space $(\mathbb{R}, \mathcal{B}(\mathbb{R}^d), \mu)$ with Borel sigma-algebra \mathcal{B} . Let $\Pi = \{\pi : \mathcal{X} \rightarrow \mathcal{U} : \pi \in C^1 \text{ and bounded}\}$ be the set of all functions from which the policy can be

²We drop $\bar{\mathbf{x}}$ from the superscript of $\mathcal{R}_\pi^{\bar{\mathbf{x}}}$, since we always assume $\bar{\mathbf{x}} = \mathbf{0}$, unless otherwise stated.

chosen. The goal can be summarized as finding a member π^* of the equivalence class of optimal policies $\Pi^* \subseteq \Pi$, where Π^* is defined as $\Pi^* = \{\pi^* \in \Pi : \mu(\mathcal{R}_{\pi^*}) = \max_{\pi \in \Pi} \mu(\mathcal{R}_{\pi})\}$. The main difficulty in this optimization problem is the fact that there is no analytical or straightforward way to infer how a change in π influences $\mu(\mathcal{R}_{\pi})$. If there exists a differentiable mapping from π to $\mu(\mathcal{R}_{\pi})$, there would be a hope to increase the stability region at least locally by perturbing the policy in the direction of $\partial\mu(\mathcal{R}_{\pi})/\partial\pi$. However, unless for extremely simple systems, such a mapping cannot be derived analytically. In this work, we construct a bridge between these two objects by an auxiliary function, which is an evolving Lyapunov function that is learned alongside the policy. Let \mathcal{D} be a domain around the equilibrium point of a closed-loop system. Due to the physical limitations of the dynamics, not every point in \mathcal{D} is stabilizable. Let $\bar{\mathcal{R}} \subseteq \mathcal{D}$ be the maximal stabilizable set within the domain \mathcal{D} . Due to space limitation, we postpone a rigorous characterization of $\bar{\mathcal{R}}$ using the concept of control Lyapunov function (clf) to Appendix A.

Our goal is to construct a sequence of policies $\{\pi_1, \pi_2, \dots\}$, such that $\mathcal{R}_{\pi_n} \xrightarrow{\mu} \bar{\mathcal{R}}$ as $n \rightarrow \infty$. This requires addressing two challenges: **1)** Approximating \mathcal{R}_{π_n} for a fixed π_n and **2)** Using (f, \mathcal{R}_{π_n}) to find π_{n+1} .

4 Proposed Method

This section addresses the two challenges mentioned at the end of Section 3. Let's define the level area of a function g with level value a as $\mathcal{S}_a(g) = \{\mathbf{x} \in \mathbb{R}^d : g(\mathbf{x}) < a\}$. The index $n \in \mathbb{N} \cup \{0\}$ refers to a stage of the algorithm. Let \mathcal{R}_{π_n} be the RoA of the closed-loop system (2) with the state-feedback policy π_n . It can be shown that there exists an optimal Lyapunov function V_{π_n} for this system with a level value c_n , such that $\mathcal{R}_{\pi_n} = \mathcal{S}_{c_n}(V_{\pi_n})$ [24]. Theoretically speaking, as c_n can be absorbed in V_{π_n} , we can keep it constant to \bar{c} and only focus on the function V_{π_n} , i.e., the information of \mathcal{R}_{π_n} is embedded in (V_{π_n}, \bar{c}) . However, in practice, c_n can take values other than \bar{c} as a result of imperfect optimization. We construct the sequence $\{\pi_1, \pi_2, \dots\}$ by an inductive process. Suppose $\Xi_n = (\pi_n, V_{\pi_n}, c_n)$ is given for $n = 0$. Constructing Ξ_{n+1} from Ξ_n is broken into two challenges mentioned at the end of Section 3. We present our proposed solution to each challenge together with their necessary assumptions and theoretical discussions in the following sections. The experiments of Section 5 show that the assumptions are not too restrictive in physical systems.

Assumption 2. Let $R : \Pi \rightarrow 2^{\mathcal{X}}$ be a set-valued function defined as $R(\pi) = \mathcal{R}_{\pi}$. Let $d_{\Pi} : \Pi \times \Pi \rightarrow \mathbb{R}_+$ and $d_{\mathcal{X}} : 2^{\mathcal{X}} \times 2^{\mathcal{X}} \rightarrow \mathbb{R}_+$ be some specified distances in the space of policies and space of all subsets of the state space, respectively. Then, the mapping R is assumed to be continuous with respect to the topologies induced by the distances d_{Π} and $d_{\mathcal{X}}$.

Verbally, this assumption means that a small change in the policy leads to a small change in the RoA induced by that policy. We show in Appendix B that Assumption 2 holds for hyperbolic systems.

Assumption 3. For two consecutive policies (π_n, π_{n+1}) , it is assumed that $\mathcal{R}_{\pi_n} \subseteq \mathcal{R}_{\pi_{n+1}}$.

The idea behind Assumption 3 is that the new policy does not forget what has been learned for stabilizing the system by the previous policy. Hence, the sequence $\{\pi_1, \pi_2, \dots\}$ gives a monotonically increasing sequence of RoAs $\{\mathcal{R}_{\pi_1}, \mathcal{R}_{\pi_2}, \dots\}$. It is convenient to show that this monotonic sequence of RoAs converges to $\bar{\mathcal{R}}$ using dominated convergence theorem [52].

Remark 4. Let $(\mathcal{R}_{\pi_{n-1}}, \pi_n)$ comprise the RoA of the previous stage and the policy of the current stage for which we want to find the RoA. Given Assumption 2, for every $\epsilon > 0$, $\delta > 0$ can be chosen small enough such that $d_{\Pi}(\pi_n, \pi_{n-1}) < \delta$ results in $\mu(\mathcal{R}_{\pi_n} \Delta \mathcal{R}_{\pi_{n-1}}) < \epsilon$.

In light of Remark 4, we assume $d_{\Pi}(\pi_n, \pi_{n-1}) < \delta$, i.e., change in policies is restricted, which means that the measure of the difference between \mathcal{R}_{π_n} and $\mathcal{R}_{\pi_{n+1}}$ is fairly small. In practice, this is guaranteed by limiting the amount of change in the parameters of the policy.

4.1 Theoretical Justification

In this section we provide a brief theoretical justification for Assumptions 2 and 3 (a more detailed exposition can be found in Appendix B). We state the results for continuous-time systems but there are similar results for discrete-time systems as well. We first need to characterize the boundary of the stability region denoted by $\partial\mathcal{R}$. Complete characterization of this boundary is not known for all nonlinear systems. Hence, we need to make an assumption about the class of considered systems.

Assumption 5. *The considered system $\dot{\mathbf{x}}(t) = f(\mathbf{x}(t))$ satisfies the following conditions: 1) All critical elements on $\partial\mathcal{R}$ are hyperbolic, 2) The stable and unstable manifolds of critical elements on $\partial\mathcal{R}$ intersect transversally (see Appendix B and [53]), and 3) Every trajectory on \mathcal{R} approaches one of the critical elements as $t \rightarrow \infty$.*

Now, we can characterize $\partial\mathcal{R}$ in terms of critical elements that lie on it.

Theorem 6 (Characterization of $\partial\mathcal{R}$: page 65 in [54]). *Suppose a closed-loop nonlinear dynamical system $\dot{\mathbf{x}}(t) = f(\mathbf{x}(t))$ satisfies Assumption 5. Let $\mathbf{x}_i, i = 1, 2, \dots$ be the equilibrium points and $\gamma_j, j = 1, 2, \dots$ be the limit cycles on $\partial\mathcal{R}$ of the asymptotically stable equilibrium point $\bar{\mathbf{x}}$. Then $\partial\mathcal{R} = \cup_i W^s(\mathbf{x}_i) \cup_j W^s(\gamma_j)$, where $W^s(y)$ is the stable manifold of the critical element y .*

A closed-loop system with a fixed controller can be seen as an autonomous system parameterized by the policy, denoted by $\dot{\mathbf{x}}(t) = f_\pi(\mathbf{x}(t))$. Therefore, updating the policy can be seen as perturbing the vector field. The qualitative changes in the behavior of dynamical systems due to the variations in the parameters of the vector field are studied under the title of *bifurcation theory*. In the following theorem, which is the main theoretical result of this paper, we prove that the policy update phase of our algorithm does not lead to a bifurcation of the RoA for hyperbolic systems, and thus, Assumption 2 is satisfied.

Theorem 7 (Persistence of the stability boundary with variations in the policy). *Consider the closed-loop hyperbolic system $\dot{\mathbf{x}}(t) = f_\pi(\mathbf{x}(t))$ with policy π . Let $(\bar{\mathbf{x}}_\pi, \mathcal{R}_\pi)$ be an asymptotically stable equilibrium point and its corresponding RoA for a certain policy $\pi = \tilde{\pi}$. Then, for every $\epsilon > 0$, there exists $\delta > 0$ such that if $d_\Pi(\tilde{\pi}, \pi') < \delta$ for a policy π' , then $\mu(\mathcal{R}_\pi \Delta \mathcal{R}_{\pi'}) < \epsilon$.*

Proof sketch. Implicit function theorem and hyperbolicity of the system is used to show that a small change in π does not lead to a large change in the stability property of critical sets. As $\partial\mathcal{R}_\pi$ is characterized by the properties of the critical elements living on it, persistence of those properties leads to the persistence of $\partial\mathcal{R}_\pi$ and consequently \mathcal{R}_π (see the detailed proof in Appendix B.1.) \square

Exact Algorithm: We describe the exact algorithm here. The practical realization comes in the next two sections. The algorithm can be seen as an iterative two-player game that alternately switches between two phases: **1) RoA estimation** and **2) Policy update**. Suppose π_n is the policy in iteration n of the algorithm. The RoA estimation phase finds a Lyapunov function V_{π_n} , such that $\mathcal{S}_{\bar{c}}(V_{\pi_n}) = \mathcal{R}_{\pi_n}$, for a fixed level value, e.g., $\bar{c} = 1$. Then, the policy update phase learns a new policy π_{n+1} , such that $\mathcal{S}_{\bar{c}}(V_{\pi_{n+1}}) = \mathcal{R}_{\pi_{n+1}}$ and $\mathcal{S}_{\bar{c}}(V_{\pi_n}) \subseteq \mathcal{S}_{\bar{c}}(V_{\pi_{n+1}})$. The change in the policy at each stage must ensure that Assumption 2 is satisfied. Moreover, the policy is regularized such that the current stable region remains stable after the policy update phase to ensure the monotonic growth of the RoA aligned with Assumption 3. As illustrated in Figure 1 the policy update phase (yellow arrows) tries to stabilize the diverging initial states (red trajectories) by pulling them towards the stable level sets of the estimated Lyapunov function. Moreover, the policy update pulls the already stabilized initial states (blue trajectories) towards the equilibrium to prevent forgetting the RoA of the previous policy. The following two phases show how the algorithm is implemented in practice.

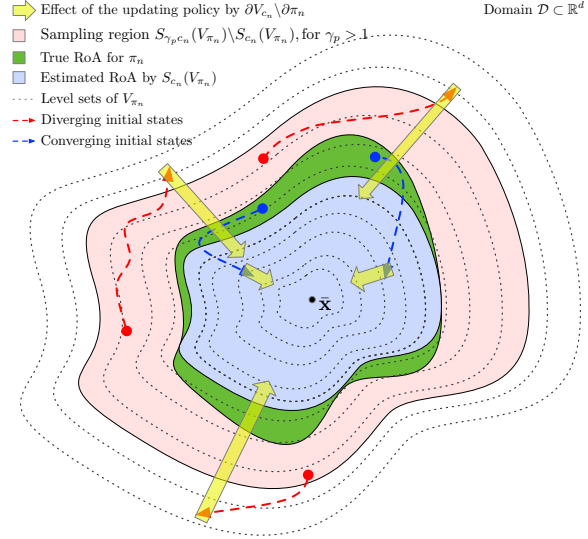


Figure 1: Illustration of the policy update phase. Given the estimated RoA, the policy update phase (yellow arrows) tries to pull the diverging trajectories starting from around the RoA towards the level sets of the estimated Lyapunov function that live inside the RoA.

4.2 RoA Estimation Phase: $(\mathcal{R}_{\pi_{n-1}}, \pi_n) \rightarrow \mathcal{R}_{\pi_n}$

This phase takes the previous policy π_{n-1} and its associated RoA estimate $\mathcal{S}_{c_{n-1}}(V_{\pi_{n-1}})$ and outputs $\mathcal{S}_{c_n}(V_{\pi_n})$ that approximates \mathcal{R}_{π_n} . We improve the *growing* algorithm proposed in [55] with the

constructive provably converging method of [56] to find a less conservative inner estimate of RoA. As stated in [55], their proposed RoA estimation algorithm is not necessarily monotonic and is prone to fall in local minima frequently. Inspired by the theoretically grounded method of [56], we added another term (weighted by λ_{monot}) to the objective function that resulted in a faster and more stable convergence to a less conservative inner estimate of the RoA (See Appendix D for the theoretical discussion). The influence of adding this new term to the objective function of [55] is empirically shown in Section 5. The learning algorithm is verbally described here while the detailed pseudo-code can be seen in Algorithm 1 in the appendix. According to Theorem 1, $\mathcal{D} = \mathcal{S}_0(\Delta f_\pi(\mathbf{x}))$ is an invariant set for the closed-loop system f_π , i.e.,

$$\text{If } \exists k_0 > 0 \text{ such that } \Phi(\mathbf{x}, k_0) \in \mathcal{D} \implies \Phi(\mathbf{x}, k) \in \mathcal{D}, \forall k > k_0 \quad (6)$$

where $\Phi(\mathbf{x}, k)$ is the system trajectory at discrete time step k . The training algorithm samples a fixed number of initial states from a gap surrounding the current estimate of RoA that is represented as a level set of a Lyapunov function. The initial states are integrated forward in time by the closed-loop dynamics to produce the solutions $\Phi(\mathbf{x}, k)$ for each initial state \mathbf{x} . The initial states are labelled based on the observation whether their solutions enter or do not enter the stable level set and construct the supervised dataset $\{\mathbb{X}^{\text{IN}}, \mathbb{X}^{\text{OUT}}\}$. The Lyapunov function is updated via the following objective function to include \mathbb{X}^{IN} as positive examples and exclude \mathbb{X}^{OUT} as negative examples in its next level set $\mathcal{S}_{c_n}(V_{\pi_n})$ where $V_{\pi_n} = \text{argmin}_V \mathcal{L}(V)$ with

$$\mathcal{L}(V) = \sum_{\mathbf{x} \in \mathbb{X}^{\text{IN}}} [V(\mathbf{x}) - \bar{c}] - \sum_{\mathbf{x} \in \mathbb{X}^{\text{OUT}}} [V(\mathbf{x}) - \bar{c}] + \lambda_{\text{RoA}} \sum_{\mathbf{x} \in \mathbb{X}^{\text{IN}}} \Delta V(\mathbf{x}) + \lambda_{\text{monot}} \sum_{\mathbf{x} \in \mathbb{X}^{\text{IN}}} [V(\mathbf{x}) - V_{\pi_{n-1}}(f_{\pi_{n-1}}(\mathbf{x}))]^2. \quad (7)$$

The first and second terms of (7) form a classification loss that separates those initial states that belong to the RoA from those that diverge. The third term encourages the negative definiteness of ΔV on the RoA. The last term is our proposed addition inspired by the constructive method of [56] that accelerates capturing the entire RoA. We assume V is chosen from the hypothesis class of positive definite functions, hence there is no need to include this condition in the optimization objective. One example of such construction is mentioned in Section 5 and is detailed in Appendix H.1.

After finding V_{π_n} by optimizing (7), the corresponding level value that gives the largest inner estimate of the RoA is not necessarily \bar{c} due to the imperfect optimization process. Hence, a line search is performed over the level values to find c_n that satisfies the conditions of Corollary 1. Sampling the initial states from the surrounding gap followed by updating the Lyapunov function repeats for a pre-determined number of steps. This process gives a sequence of sets that starts from $\mathcal{R}_{\pi_{n-1}}$ represented by $(V_{\pi_{n-1}}, c_{n-1})$ and gets closer and closer to \mathcal{R}_{π_n} represented by (V_{π_n}, c_n) . See Algorithm 1 in the appendix for the detailed presentation.

4.3 Policy Update: $\mathcal{R}_{\pi_n} \rightarrow \pi_{n+1}$

This phase of the algorithm uses the information (V_{π_n}, c_n) to update the policy so that the new policy gives rise to a larger stability region. The policy is changed such that some of the diverging initial states around the current RoA converge towards the RoA. Let \mathcal{D} be a domain around the equilibrium $\bar{\mathbf{x}}$. Given a hypothesis class of feasible policies Π , only a subset of the domain \mathcal{D} is stabilizable (see Equation (11) in Appendix A). Assume $\tilde{\mathcal{B}} \subseteq \mathcal{D}$ is the maximum stabilizable subset of the domain with $\mu(\tilde{\mathcal{B}}) = \bar{\mu}$. Therefore, an attempt to improve π_n amounts to appending points from $\tilde{\mathcal{B}} \setminus \mathcal{R}_{\pi_n}$ to \mathcal{R}_{π_n} . The set $\tilde{\mathcal{B}}$ is not fully known in advance but some of its properties can be derived.

Lemma 8. [54] *For the system (1), if $f, \pi \in C^\infty$, the maximum stabilizable set $\tilde{\mathcal{B}}$ whose measure materializes as $\bar{\mu}$ is compact and connected.*

In light of Lemma 8, if $\mathcal{R}_{\pi_n} \subset \tilde{\mathcal{B}}$, the stabilizable states can be chosen in a gap around \mathcal{R}_{π_n} . As \mathcal{R}_{π_n} is represented via (V_{π_n}, c_n) , a gap can be constructed as $\mathcal{G}_n = \mathcal{S}_{\gamma_p c_n}(V_{\pi_n}) \setminus \mathcal{S}_{c_n}(V_{\pi_n})$ for a $\gamma_p > 1$. To make sure the policy does not forget the already stable region, the algorithm also samples initial states from $\mathcal{S}_{c_n}(V_{\pi_n})$. The initial states are integrated forward for L_p steps and the policy is updated via minimizing the following objective function in order to encourage $V_{\pi_n}(\Phi_\pi(\mathbf{x}, L_p)) < c_n$ for the stabilizable states.

$$\mathcal{L}(\pi) = \sum_{\mathbf{x} \in \mathcal{G}_n \cup \mathcal{S}_{c_n}(V_{\pi_n})} V_{\pi_n}(\Phi_\pi(\mathbf{x}, L_p)) \mathbb{1}_{[V_{\pi_n}(\Phi_\pi(\mathbf{x}, L_p)) < c_n]} + \lambda_u \sum_{\mathbf{x} \in \mathcal{G}_n} V_{\pi_n}(\Phi_\pi(\mathbf{x}, L_p)) \mathbb{1}_{[V_{\pi_n}(\Phi_\pi(\mathbf{x}, L_p)) > c_n]} \quad (8)$$

Notice that $\Phi_\pi(\mathbf{x}, L_p)$ is the trajectory of the closed-loop system with the trainable policy π . The first term makes sure the new policy does not destabilize the currently stable states. We observed

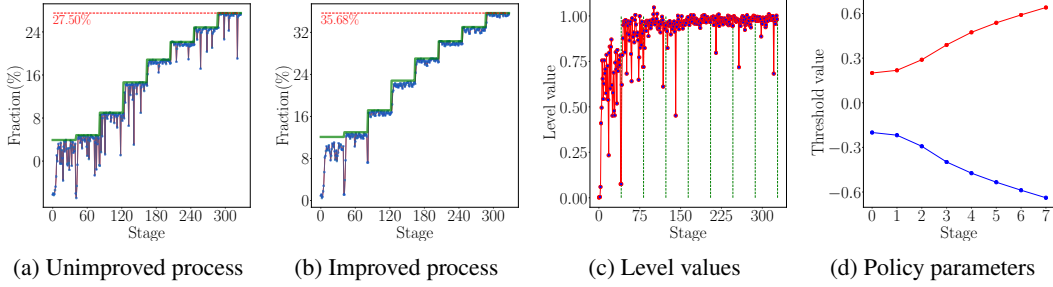


Figure 2: (a), (b) The size of the RoA against the iterative stages of the Algorithms 4.2 and 4.3 where (a) uses the RoA estimation method of [55] while (b) uses ours. The fraction is computed with respect to a rectangular domain around the equilibrium point that is large enough to enclose the RoA. Green: size of the true RoA. Each jump corresponds to a policy update that increases the size of the true RoA. Red: The size of the RoA estimated by Algorithm 4.2. After each policy update, the RoA estimation algorithm takes multiple growth steps to capture the true RoA as close as it can. (c) The trace of the level values corresponding to every iteration of the RoA estimation algorithm. (d) Red (Blue): The trace of the value of the upper (lower) threshold during training. Each point corresponds to a policy update iteration.

empirically that the inclusion of this term facilitates the satisfaction of Assumption 3 and results in a more monotonic policy improvement. The second term tries to make the diverging initial states converge to the equilibrium and consequently enlarges the RoA. The weighting factor λ_u is chosen larger than 1 to put more emphasis on stabilizing the unstable initial states. The detailed pseudo-code of this phase can be found in Algorithm 2 in the appendix. One critical hyper-parameter of this phase is L_p that is the length of the produced trajectory. The following remark elaborates more on the effect of this hyper-parameter on learning signals.

Remark 9 (Length of the trajectories). *The policy π affects the loss function $\mathcal{L}(\pi)$ only via the Lyapunov function V as can be seen in (8). Because the Lyapunov function itself is learned by the other phase of the algorithm in Section 4.2, an ill-conditioned V can harm the policy update phase. For example, an almost flat V at the location of $\Phi_\pi(\mathbf{x}, L_p)$ weakens the training signal $\partial\mathcal{L}/\partial\pi$. Hence, a too-long trajectory will be either dangerous or unhelpful. It will be dangerous for unstable initial states as it may grow unboundedly and damage the system. Likewise, it will be unhelpful for stable initial states because $\nabla_{\mathbf{x}}V(\mathbf{x})$ is a continuous function that vanishes at the equilibrium point, i.e., it takes vanishing values in a neighborhood of the equilibrium (we prove this point as a lemma in the appendix, see Lemma 11). The vanishing gradient of the Lyapunov function results in the vanishing gradient for the policy parameters, that in turn gives rise to a weak learning signal. An extensive theoretical investigation of the vanishing gradient issue is presented in Appendix G.*

The following remark discusses to what extent the model of the system is needed.

Remark 10. *The RoA estimation phase does not need the model of the system. The system can be launched from sampled initial states and the generated trajectories are all we need in (7). The policy update phase of the algorithm requires a local estimate of the system to be able to compute $\partial V/\partial\pi$. The locality of the model is inversely proportional to the length of the trajectory L_p in (8). A detailed theoretical discussion on this point is deferred to Appendix F.*

5 Experiments

We consider an inverted pendulum system defined as $\dot{\theta} = \omega$ and $\dot{\omega} = \frac{g}{l} \sin(\theta) + \frac{u}{I} - \mu_f \frac{\omega}{I}$ where the state vector $\mathbf{x} = (\theta, \omega)$ consists of the angle and angular velocity. Moreover ($g = 0.81, l = 0.5, I = \text{mass} \times l^2 = 0.25, \mu_f = 0$) are the acceleration of gravity, length, inertia, and friction coefficient. The scalar u is the input force. The open-loop system (with $u = 0$) has equilibrium points at $(\theta, \omega) = (k\pi, 0)$ with $k \in \mathbb{Z}$. We focus on the equilibrium point $(0, 0)$ in the frictionless setting where the system shows oscillatory behavior and consequently is not asymptotically stable. As an initial step, an LQR

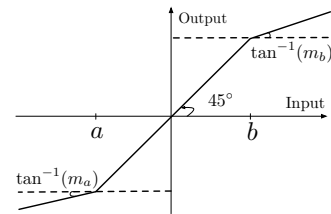


Figure 3: Loose saturation

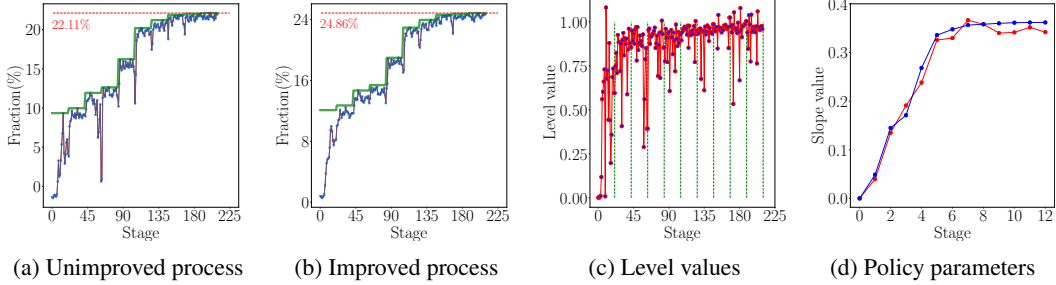


Figure 4: The same plots as Figure 2 with the exception that, here the thresholds are kept fixed at $a = 0.2$ and $b = -0.2$ while the slopes m_a and m_b are trainable parameters.

controller K is designed for the linearized system around the origin (see the vector field and the initial RoA in Figure 6 in the appendix). The control signal at stage 0 passes through a loose saturation function as $u = \pi_0(\mathbf{x}; \psi) = \text{SAT}_\psi([\theta, \omega]^T K)$. The function SAT is parameterized by $\psi = (a, b, m_a, m_b)$ as illustrated in Figure 3. In the first experiment, the slopes $m_a = 0$ and $m_b = 0$ are kept fixed where a and b are trainable parameters of the policy, i.e., $\psi = (a, b)$. The Lyapunov function $V(\cdot; \theta)$ is realized by a 3-layer neural network parameterized by θ . Each layer has 64 neurons with a special structure (see Appendix H.1) followed by tanh activation function that imposes the positive definiteness of the entire network as is required by Equation (4) and Section 4.2. The training details and the chosen hyper-parameters can be found in Appendix H.

The initial controller gives a small RoA since it is designed for the local linear approximation of the system. As the initial policy is LQR designed for the locally linearized model, $V(\cdot; \theta)$ is pre-trained by the quadratic function $0.1\theta^2 + 0.1\omega^2$. We found the pre-training step important as the level sets of a randomly initialized network can be quite complex and far from the shape of the RoA that it aims to approximate. After pre-training, the algorithms of Sections 4.2 and 4.3 are run alternately to capture the RoA and improve the policy. The green step-like plot in Figure 2a and Figure 2b shows the true size of the RoA. Each jump in the green plots shows one iteration of the policy update algorithm resulting in an increased RoA. The fluctuating red plot in Figure 2a shows the size of the estimated RoA by Section 4.2 without our improvement over the RoA estimation algorithm of [55] while Figure 2b shows the outcome of the presence of our proposed additional term in the objective function. It shows that the added term results in a less fluctuating estimate of the RoA, and when combined with the policy update phase, gives a faster convergence to a larger RoA (35.68% vs 27.50% fraction of the domain volume after 7 policy updates).

As stated in Section 4.2, c_n is not necessarily the desired \bar{c} . Here we set $\bar{c} = 1$ and find the value of c_n at each iteration such that the conditions of Corollary 1 are met. It can be seen in Figure 2c that these values converge to $\bar{c} = 1$ that can be perceived as a sign of the stable training of the algorithm.

The trace of the parameters of the policy is shown in Figure 2d. As these policy’s trainable parameters represent the upper and lower limits of the loose threshold function, the policy learning algorithm updates them in the directions that decrease their suppressing effect. This is what we also expect from the physics of the system. Graphical visualization of the policy update and RoA estimation phase is shown in Figure 5. The policies are updated along the rows from top to bottom. Within one row, the policy is fixed and RoA is estimated from left to right (See Figure 8 in the appendix for a larger visualization).

In the second experiment, the threshold limits $a = -0.2$ and $b = 0.2$ are kept fixed while the slopes $\psi = (m_a, m_b)$ are trainable parameters. The rest of the training setting remains the same as the

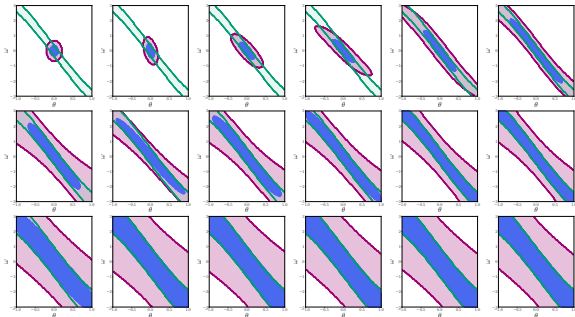


Figure 5: Visualizing the true RoA which is enlarged by the improved policy and is chased by a learned Lyapunov function. Green boundary: True RoA, Blue: $S_{c_n}(V_{\pi_n})$, Pink: $S_{\gamma c_n}(V_{\pi_n})$ for $\gamma = 4$. The pink area shows the region from which the samples outside the estimated RoA is taken for both estimating the RoA and updating the policy.

previous experiment. Figures 4a and 4b shows that the policy update phase enlarges the RoA (green plot) of the system while the RoA estimation phase (red plot) manages to follow the new RoA after each policy update. Our improved RoA estimation algorithm results in a more monotonic convergence of the estimated RoA that ultimately learns a controller with a larger RoA (24.86% vs 22.11%). Similar to Figure 2c, convergence of c_n values to $\bar{c} = 1$ can be seen in Figure 4c. The trace of the upper and lower slopes are shown in Figure 4d. Almost equal learned values for upper and lower slopes are expected due to the physical symmetry of the closed-loop system.

6 Related Work and Conclusions

The existing approaches most comparable to the idea of this paper are those that simultaneously synthesize a controller and maximize the stability region. Sums-of-squares (SOS) is used for polynomial systems and leads to a bilinear optimization that is solved by some form of alternation [57, 58]. As a dual to Lyapunov-based methods, [59] uses the notion of occupation measure to optimize a feedback controller for a polynomial system, but it has scalability issues due to its reliance on SDP optimization toolbox. Our work is different from this class of methods as our method is not limited to polynomial systems. Moreover, our method uses automatic differentiation that is naturally combined with neural networks to enjoy their superior scalability. A more data-driven approach is adopted in [60] that uses statistical models of the system to learn a controller with the assumption that the Lyapunov function is given. Our method is different from this work as we learn the Lyapunov function and the controller together in an alternating fashion. In the context of reinforcement learning, our method can be seen as an actor-critic approach [61–63] where the actor tries to stabilize the system while the critic estimates the size of the RoA induced by the controller. Despite mostly differentiable critics in reinforcement learning algorithms, here we had to use a Lyapunov function as a mediator to build a differentiable map between the actor and the critic.

We have proposed a two-player collaborative iterative algorithm that iterates over two phases. In one phase, the RoA of the closed-loop system is estimated by learning a Lyapunov function. In the other phase, estimated information of the first phase is used to update the policy to one with a larger RoA. Despite classical methods in control theory, this alternating approach frees us from analytical and expression-level controller synthesis as it relies on automatic differentiation and the back-propagation of error through trajectories of the system. In this work, we assumed the model of the system is given, however, as it was mentioned in Remark 10, the first phase can be done model-free and the required model of the system can be learned locally in the second phase. Investigating this direction further is deferred to future work.

References

- [1] F Liao and JL Wang. Analysis and synthesis of reliable flight control systems via parameter-dependent lyapunov functions. *Proceedings of the Institution of Mechanical Engineers, Part I: Journal of Systems and Control Engineering*, 218(6):433–450, 2004.
- [2] Chiharu Ishii, Hiroyuki Mikami, and Yosuke Nishitani. Lyapunov-based bilateral teleoperation for surgical robotic forceps system with time varying delay. *International Journal of Mechatronics and Automation*, 2(2):132–146, 2012.
- [3] Zhu Wen-Xing and Zhang Li-Dong. A new car-following model for autonomous vehicles flow with mean expected velocity field. *Physica A: Statistical Mechanics and its Applications*, 492:2154–2165, 2018.
- [4] Harry A Pierson and Michael S Gashler. Deep learning in robotics: a review of recent research. *Advanced Robotics*, 31(16):821–835, 2017.
- [5] Hsiao-Dong Chang, Chia-Chi Chu, and Gerry Cauley. Direct stability analysis of electric power systems using energy functions: theory, applications, and perspective. *Proceedings of the IEEE*, 83(11):1497–1529, 1995.
- [6] H Xin, D Gan, J Qiu, and Z Qu. Methods for estimating stability regions with applications to power systems. *European transactions on electrical power*, 17(2):113–133, 2007.
- [7] Kenneth L Praprost and Kenneth A Loparo. A stability theory for constrained dynamic systems with applications to electric power systems. *IEEE transactions on Automatic Control*, 41(11):1605–1617, 1996.
- [8] Joao Manoel Gomes da Silva Jr, Sophie Tarbouriech, and Germain Garcia. Anti-windup design for time-delay systems subject to input saturation an lmi-based approach. *European Journal of Control*, 12(6):622–634, 2006.
- [9] Bernd Tibken. Estimation of the domain of attraction for polynomial systems via lmis. In *Proceedings of the 39th IEEE Conference on Decision and Control (Cat. No. 00CH37187)*, volume 4, pages 3860–3864. IEEE, 2000.
- [10] H Xin, D Gan, M Huang, and K Wang. Estimating the stability region of singular perturbation power systems with saturation nonlinearities: an linear matrix inequality-based method. *IET control theory & applications*, 4(3):351–361, 2010.
- [11] K Ciliz and A Harova. Stability regions of recurrent type neural networks. *Electronics Letters*, 28(11):1022–1024, 1992.
- [12] John J Hopfield. Neurons, dynamics and computation. *Physics Today*, 47(2):40–47, 1994.
- [13] Eric R Westervelt, Jessy W Grizzle, and C Canudas De Wit. Switching and pi control of walking motions of planar biped walkers. *IEEE Transactions on Automatic Control*, 48(2):308–312, 2003.
- [14] Eric R Westervelt, Jessy W Grizzle, and Daniel E Koditschek. Hybrid zero dynamics of planar biped walkers. *IEEE transactions on automatic control*, 48(1):42–56, 2003.
- [15] Steven M Baer, Bingtuan Li, and Hal L Smith. Multiple limit cycles in the standard model of three species competition for three essential resources. *Journal of mathematical biology*, 52(6):745–760, 2006.
- [16] Elena Glassman, Alexis Lussier Desbiens, Mark Tobenkin, Mark Cutkosky, and Russ Tedrake. Region of attraction estimation for a perching aircraft: A lyapunov method exploiting barrier certificates. In *2012 IEEE International Conference on Robotics and Automation*, pages 2235–2242. IEEE, 2012.
- [17] Marian Anghel, Federico Milano, and Antonis Papachristodoulou. Algorithmic construction of lyapunov functions for power system stability analysis. *IEEE Transactions on Circuits and Systems I: Regular Papers*, 60(9):2533–2546, 2013.

- [18] Mehdi Imani Masouleh and David JN Limebeer. Region of attraction analysis for nonlinear vehicle lateral dynamics using sum-of-squares programming. *Vehicle System Dynamics*, 56(7):1118–1138, 2018.
- [19] Alberto Isidori. *Nonlinear Control Systems Design 1989: Selected Papers from the IFAC Symposium, Capri, Italy, 14-16 June 1989*. Elsevier, 2014.
- [20] Hassan K Khalil and Jessy W Grizzle. *Nonlinear systems*, volume 3. Prentice hall Upper Saddle River, NJ, 2002.
- [21] Mathukumalli Vidyasagar. *Nonlinear systems analysis*, volume 42. Siam, 2002.
- [22] Alan SI Zinober. Deterministic control of uncertain systems. In *Proceedings. ICCON IEEE International Conference on Control and Applications*, pages 645–650. IEEE, 1989.
- [23] Roberto Genesio, Michele Tartaglia, and Antonio Vicino. On the estimation of asymptotic stability regions: State of the art and new proposals. *IEEE Transactions on automatic control*, 30(8):747–755, 1985.
- [24] Anthony Vannelli and Mathukumalli Vidyasagar. Maximal lyapunov functions and domains of attraction for autonomous nonlinear systems. *Automatica*, 21(1):69–80, 1985.
- [25] Alexandre Liapounoff. Problème général de la stabilité du mouvement. In *Annales de la Faculté des sciences de Toulouse: Mathématiques*, volume 9, pages 203–474, 1907.
- [26] Joseph LaSalle. Some extensions of liapunov’s second method. *IRE Transactions on circuit theory*, 7(4):520–527, 1960.
- [27] Yuandan Lin, Eduardo D Sontag, and Yuan Wang. A smooth converse lyapunov theorem for robust stability. *SIAM Journal on Control and Optimization*, 34(1):124–160, 1996.
- [28] Eduardo D Sontag. A lyapunov-like characterization of asymptotic controllability. *SIAM journal on control and optimization*, 21(3):462–471, 1983.
- [29] Z Arstein. Stabilization with relaxed controls. *Nonlinear analysis*, 7(11):1163–1173, 1983.
- [30] Randy Freeman and Petar V Kokotovic. *Robust nonlinear control design: state-space and Lyapunov techniques*. Springer Science & Business Media, 2008.
- [31] Christopher M Bishop. *Pattern recognition and machine learning*. springer, 2006.
- [32] Vladimir Vapnik. *The nature of statistical learning theory*. Springer science & business media, 2013.
- [33] Zhong-Sheng Hou and Zhuo Wang. From model-based control to data-driven control: Survey, classification and perspective. *Information Sciences*, 235:3–35, 2013.
- [34] Gianluigi Pillonetto, Francesco Dinuzzo, Tianshi Chen, Giuseppe De Nicolao, and Lennart Ljung. Kernel methods in system identification, machine learning and function estimation: A survey. *Automatica*, 50(3):657–682, 2014.
- [35] S Reynold Chu, Rahmat Shoureshi, and Manoel Tenorio. Neural networks for system identification. *IEEE Control systems magazine*, 10(3):31–35, 1990.
- [36] Friedrich Solowjow, Arash Mehrjou, Bernhard Schölkopf, and Sebastian Trimpe. Minimum information exchange in distributed systems. In *57th IEEE Conference on Decision and Control (CDC)*. [Electronic resource], 2018.
- [37] Arash Mehrjou, Friedrich Solowjow, Sebastian Trimpe, and Bernhard Schölkopf. A local information criterion for dynamical systems. *arXiv preprint arXiv:1805.10615*, 2018.
- [38] Samuel Greydanus, Misko Dzamba, and Jason Yosinski. Hamiltonian neural networks. In *Advances in Neural Information Processing Systems*, pages 15353–15363, 2019.
- [39] Arash Mehrjou and Bernhard Schölkopf. Deep lyapunov function: Automatic stability analysis for dynamical systems. *arXiv preprint arXiv:1901.08403*, 2019.

- [40] Arash Mehrjou and Bernhard Schölkopf. Deep nonlinear non-gaussian filtering for dynamical systems. *arXiv preprint arXiv:1811.05933*, 2018.
- [41] Ian Goodfellow, Jean Pouget-Abadie, Mehdi Mirza, Bing Xu, David Warde-Farley, Sherjil Ozair, Aaron Courville, and Yoshua Bengio. Generative adversarial nets. In *Advances in neural information processing systems*, pages 2672–2680, 2014.
- [42] Arash Mehrjou and Bernhard Schölkopf. Nonstationary gans: Analysis as nonautonomous dynamical systems. In *Workshop on Theoretical Foundations and Applications of Deep Generative Models at ICML*, 2018.
- [43] Arash Mehrjou. Analysis of nonautonomous adversarial systems. *arXiv preprint arXiv:1803.05045*, 2018.
- [44] Lars Mescheder, Sebastian Nowozin, and Andreas Geiger. The numerics of gans. In *Advances in Neural Information Processing Systems*, pages 1825–1835, 2017.
- [45] Arash Mehrjou, Wittawat Jitkrittum, Krikamol Muandet, and Bernhard Schölkopf. Kernel-guided training of implicit generative models with stability guarantees. *arXiv preprint arXiv:1910.14428*, 2019.
- [46] David Balduzzi, Sebastien Racaniere, James Martens, Jakob Foerster, Karl Tuyls, and Thore Graepel. The mechanics of n-player differentiable games. *arXiv preprint arXiv:1802.05642*, 2018.
- [47] Sai Ganesh Nagarajan, David Balduzzi, and Georgios Piliouras. Robust self-organization in games: Symmetries, conservation laws and dimensionality reduction. In *Proceedings of the 19th International Conference on Autonomous Agents and MultiAgent Systems*, pages 1946–1948, 2020.
- [48] David Berthelot, Thomas Schumm, and Luke Metz. Began: Boundary equilibrium generative adversarial networks. *arXiv preprint arXiv:1703.10717*, 2017.
- [49] J Jr Palis and Welington De Melo. *Geometric theory of dynamical systems: an introduction*. Springer Science & Business Media, 2012.
- [50] Victor Guillemin and Alan Pollack. *Differential topology*, volume 370. American Mathematical Soc., 2010.
- [51] Donald E Kirk. *Optimal control theory: an introduction*. Courier Corporation, 2004.
- [52] Heinz Bauer. *Measure and integration theory*, volume 26. Walter de Gruyter, 2011.
- [53] Manfredo P Do Carmo. *Differential geometry of curves and surfaces: revised and updated second edition*. Courier Dover Publications, 2016.
- [54] Hsiao-Dong Chiang and Luís FC Alberto. *Stability regions of nonlinear dynamical systems: theory, estimation, and applications*. Cambridge University Press, 2015.
- [55] Spencer M Richards, Felix Berkenkamp, and Andreas Krause. The lyapunov neural network: Adaptive stability certification for safe learning of dynamic systems. *arXiv preprint arXiv:1808.00924*, 2018.
- [56] H-D Chiang and James S Thorp. Stability regions of nonlinear dynamical systems: A constructive methodology. *IEEE Transactions on Automatic Control*, 34(12):1229–1241, 1989.
- [57] Zachary Jarvis-Wloszek, Ryan Feeley, Weehong Tan, Kunpeng Sun, and Andrew Packard. Some controls applications of sum of squares programming. In *42nd IEEE international conference on decision and control (IEEE Cat. No. 03CH37475)*, volume 5, pages 4676–4681. IEEE, 2003.
- [58] Anirudha Majumdar, Amir Ali Ahmadi, and Russ Tedrake. Control design along trajectories with sums of squares programming. In *2013 IEEE International Conference on Robotics and Automation*, pages 4054–4061. IEEE, 2013.

- [59] Anirudha Majumdar, Ram Vasudevan, Mark M Tobenkin, and Russ Tedrake. Convex optimization of nonlinear feedback controllers via occupation measures. *The International Journal of Robotics Research*, 33(9):1209–1230, 2014.
- [60] Felix Berkenkamp, Matteo Turchetta, Angela Schoellig, and Andreas Krause. Safe model-based reinforcement learning with stability guarantees. In *Advances in neural information processing systems*, pages 908–918, 2017.
- [61] Ivo Grondman, Lucian Busoniu, Gabriel AD Lopes, and Robert Babuska. A survey of actor-critic reinforcement learning: Standard and natural policy gradients. *IEEE Transactions on Systems, Man, and Cybernetics, Part C (Applications and Reviews)*, 42(6):1291–1307, 2012.
- [62] Shubhendu Bhasin, Rushikesh Kamalapurkar, Marcus Johnson, Kyriakos G Vamvoudakis, Frank L Lewis, and Warren E Dixon. A novel actor–critic–identifier architecture for approximate optimal control of uncertain nonlinear systems. *Automatica*, 49(1):82–92, 2013.
- [63] Timothy P Lillicrap, Jonathan J Hunt, Alexander Pritzel, Nicolas Heess, Tom Erez, Yuval Tassa, David Silver, and Daan Wierstra. Continuous control with deep reinforcement learning. *arXiv preprint arXiv:1509.02971*, 2015.
- [64] Philip Hartman. A lemma in the theory of structural stability of differential equations. *Proceedings of the American Mathematical Society*, 11(4):610–620, 1960.
- [65] David M Grobman. Homeomorphism of systems of differential equations. *Doklady Akademii Nauk SSSR*, 128(5):880–881, 1959.
- [66] Steven G Krantz and Harold R Parks. *The implicit function theorem: history, theory, and applications*. Springer Science & Business Media, 2012.

A Control Lyapunov Function and Maximal Stabilizable Set

The use of the Lyapunov theory to guide designing the input of a system has been made precise with the introduction of *control Lyapunov function (clf)*. A clf for a system of the form $\mathbf{x}_{k+1} = f(\mathbf{x}_k, \mathbf{u}_k)$ is a C^1 , radially unbounded function $V : \mathcal{X} \rightarrow \mathbb{R}_+$ if

$$V(\mathbf{0}) = 0 \quad \text{and} \quad V(\mathbf{x}) > 0 \quad \forall \mathbf{x} \in \mathcal{D} \setminus \{\mathbf{0}\} \quad (9)$$

$$\inf_{\mathbf{u} \in U} [V(\mathbf{x}) - V(f(\mathbf{x}, \mathbf{u}))] \leq 0 \quad \forall \mathbf{x} \in \mathcal{D} \setminus \{\mathbf{0}\} \quad (10)$$

Just as the existence of the lf is necessary and sufficient conditions for the stability of an autonomous system, the existence of a clf is a necessary and sufficient condition for *stabilizability* of a system with control input. In other words, the existence of clf guarantees the existence of a controller that stabilizes the system for all initial states within a neighborhood around the equilibrium point.

According to the definition of lf in Section 2 and clf above, lf assess the stability of a closed-loop system for a fixed controller while clf shows if there *exists* a control signal that stabilizes the system in a domain \mathcal{D} . In the definition of clf, no functional limitation is assumed for the control signal $\mathbf{u}(t)$. In practice, $\mathbf{u}(t)$ is produced by a state-feedback controller via the policy function $\pi \in \Pi$. Moreover, due to the implementation limits, only a subset $\tilde{\Pi} \subseteq \Pi$ of these functions can be realized. Therefore, it is quite likely that $\mu(\mathcal{R}_{\pi^*}) < \mu(\mathcal{D})$, i.e., the best feasible controller cannot expand the RoA of the system to the entire \mathcal{D} . Let $U(\mathbf{x})$ be the values that the control signal can take at state \mathbf{x} . Then, we define

$$\bar{\mathcal{R}} = \sup_{\mathcal{B} \subseteq \mathcal{D}} \mathcal{B} \quad \text{such that} \quad \exists \text{ clf } V \text{ on } \mathcal{B} \text{ and a } \pi \in \tilde{\Pi} \text{ with } U(\mathbf{x}) = \pi(\mathbf{x}), \forall \mathbf{x} \in \mathcal{B} \quad (11)$$

where $\bar{\mathcal{R}}$ is the maximal stabilizable set as was used in Section 3. In this definition, the constraints on the control signal is also taken into account using the set-valued function $U(\mathbf{x})$.

B More Detailed Theoretical Discussions

In this section, we take a closer look at the potential challenges of the method proposed in Section 4 from a theoretical perspective. The purpose of the proposed algorithm is to improve the controller with the goal of enlarging the stability region of the system. Similar to any other nonlinear control strategy, the method cannot be applied to all nonlinear systems. In the following, we characterize the systems that can be approached by the proposed method.

According to Assumption 2 and Remark 4, updating the controller at each stage must not change the RoA drastically. This guarantees a smooth gradual improvement of the policy while, at the same time, the Lyapunov function of the previous stage is a fine initialization for the Lyapunov function of the next stage. To obtain a deeper insight into this assumption, we need to characterize the stability boundary induced by the policy π that is denoted by $\partial \mathcal{R}_\pi$. We present the results for the continuous-time system while similar results can be derived for discrete-time systems as well.

Consider the autonomous nonlinear dynamical system $\dot{\mathbf{x}}(t) = f(\mathbf{x}(t))$. Recall from Section 2 that an equilibrium point $\bar{\mathbf{x}}$ of this system is *hyperbolic* if the corresponding Jacobian matrix $J_f(\bar{\mathbf{x}})$ has no eigenvalues with zero real-part. As a consequence of implicit function theorem, hyperbolic equilibrium points are isolated and also have properties that facilitate dealing with them. Hartman-Grobman theorem ensures that the stability properties of a hyperbolic equilibrium point is the same as its linearization [64, 65]. This can be shown by constructing a homeomorphism between trajectories of the nonlinear system and its linear counterpart in a vicinity around the equilibrium. Similar results can be proved for other invariant manifolds such as limit cycles. Hartman-Grobman theorem also shows via *stable manifold theorem* that the state space can be decomposed into stable and unstable manifolds around a hyperbolic invariant set. The trajectories in each of these manifolds have the same stability properties as the trajectories in the corresponding eigenspace of the linearized system. Moreover, $\bar{\mathbf{x}} \in \mathbb{R}^n$ is said to be a type- k equilibrium point if $\dim(W^u(\bar{\mathbf{x}})) = k$ and $\dim(W^s(\bar{\mathbf{x}})) = n - k$. This is the result of a more general property that the stable and unstable manifolds of a hyperbolic equilibrium point intersect *transversely*. Roughly speaking *transversality* condition ensures that the manifolds intersect in a generic way (See any book on differential geometry such as [53] for a more concrete exposition of transversality). To characterize the boundary of RoA

($\partial\mathcal{R}$), we introduce Assumption 5 that allows us to characterize $\partial\mathcal{R}$ in terms of the critical elements that lie on it according to Theorem 6.

A closed-loop system with a fixed controller can be seen as an autonomous system parameterized by the policy denoted by $\dot{\mathbf{x}}(t) = f_\pi(\mathbf{x}(t))$. Therefore, the policy update (Algorithm 2) can be seen as perturbing the vector field f_π . The qualitative changes in the behavior of dynamical systems due to variations in the parameters of the vector field are studied under the title *bifurcation theory*. Bifurcation in RoA due to the perturbation caused by the policy update can significantly impact its shape and size which is a fundamental concern in our algorithm and many other applications that rely on a smooth change of the RoA with respect to the vector field.

B.1 Proof of Theorem 7

In this section we restate Theorem 7 and provide a more detailed proof.

Theorem (Persistence of the stability boundary with variations in the policy). *Consider the closed-loop hyperbolic system $\dot{\mathbf{x}}(t) = f_\pi(\mathbf{x}(t))$ with policy π . Let $(\bar{\mathbf{x}}_{\tilde{\pi}}, \mathcal{R}_{\tilde{\pi}})$ be an asymptotically stable equilibrium point and its corresponding RoA for a certain policy $\pi = \tilde{\pi}$. Then, for every $\epsilon > 0$, there exists $\delta > 0$ such that if $d_\Pi(\tilde{\pi}, \pi') < \delta$, then $\mu(\mathcal{R}_{\tilde{\pi}} \triangle \mathcal{R}_{\pi'}) < \epsilon$.*

Proof. As $\mathcal{R}_{\tilde{\pi}}$ is characterized by its boundary, we turn our attention to $\partial\mathcal{R}_{\tilde{\pi}}$. As a result of the continuity of $f(\mathbf{x}, \mathbf{u})$ and $\pi(\mathbf{x})$ with respect to their arguments, implicit function theorem guarantees that small perturbations to $\tilde{\pi}$ causes small changes to hyperbolic equilibrium points [66]. Formally speaking, if $\mathbf{x}_{\tilde{\pi}}^*$ is a hyperbolic equilibrium point of $\dot{\mathbf{x}}(t) = f_\pi(\mathbf{x}(t))$ for $\pi = \tilde{\pi}$, there exists a $\delta > 0$ and a neighborhood U of $\mathbf{x}_{\tilde{\pi}}^*$ such that the closed-loop system has a unique hyperbolic equilibrium point $\mathbf{x}_{\pi'}^*$, for every $\pi' \in \{\pi \in \Pi : d_\Pi(\pi, \tilde{\pi}) < \delta\}$. Moreover, the continuity of the eigenvalues of $J_{f_\pi}(\mathbf{x}_{\pi'})$ with respect to π affirms that the perturbed equilibrium point $\mathbf{x}_{\pi'}^*$ has the same stability condition as $\mathbf{x}_{\tilde{\pi}}^*$, i.e., there exists a homeomorphism $h : \mathbb{R}^n \rightarrow \mathbb{R}^n$ from $\Phi_{\tilde{\pi}}(\mathbf{x}, t)$ to $\Phi_{\pi'}(\mathbf{x}, t)$. As stated by Theorem 6, $\partial\mathcal{R}_{\tilde{\pi}}$ is characterized by the stable manifolds of unstable equilibrium points living on the boundary. Hence the hyperbolic equilibrium points on $\partial\mathcal{R}_{\tilde{\pi}}$ together with their stable and unstable manifolds change continuously with $\tilde{\pi}$. This results in a continuous change of $\partial\mathcal{R}_{\tilde{\pi}}$ and consequently $\mathcal{R}_{\tilde{\pi}}$ with respect to variations in $\tilde{\pi}$. \square

C Other Proofs

In this section, a more detailed theoretical exposition of some of the material that is dropped from the main text is presented.

The following lemma shows that the derivative of a Lyapunov function vanishes at the equilibrium point. In an actor-critic view to our proposed algorithm, the Lyapunov function plays the role of the critic. As the learning signal for updating the actor (policy) passes through the derivative of the critic (Lyapunov function) due to the chain rule, the following lemma implies that getting closer to the equilibrium will weaken the information content of the signal for learning the policy.

Lemma 11. *Derivative of a Lyapunov function at the origin: Let $\mathcal{X} \subseteq \mathbb{R}^d$ be a d -dimensional vector space and $V : \mathcal{X} \rightarrow \mathbb{R}$ be a continuous positive definite function, i.e., $V(\mathbf{x}) > 0$ for $\mathbf{x} \neq \mathbf{0}$ and $V(\mathbf{0}) = 0$. Then, $\nabla_{\mathbf{x}} V(\mathbf{x})|_{\mathbf{x}=\mathbf{0}} = 0$.*

Proof. We use the technique of proof by contradiction. Let $\mathbf{g} = [g_1, g_2, \dots, g_d]^T = \nabla_{\mathbf{x}} V(\mathbf{x})|_{\mathbf{x}=\mathbf{0}} \neq 0$. Suppose there exists an index $i \in \{1, 2, \dots, d\}$ such that $g_i \neq 0$. Due to the continuity of V , we expand $V(\mathbf{x})$ at $\mathbf{x} = \mathbf{0}$ in the direction of g_i as

$$V(0, \dots, x_i = c, \dots, 0) = V(\mathbf{0}) + c \frac{\partial V(\mathbf{x})}{\partial x_i} \Big|_{\mathbf{x}=\mathbf{0}} + o(x_i)$$

for an arbitrary value of c close to 0. Since c is arbitrary, we choose $c = -\epsilon \frac{\partial V(\mathbf{x})}{\partial x_i} \Big|_{\mathbf{x}=\mathbf{0}} = -\epsilon g_i$. As we assumed $V(\mathbf{0}) = 0$, for ϵ sufficiently close to 0, we can write

$$V(0, \dots, x_i = c, \dots, 0) = -\epsilon g_i^2 < 0 \text{ for } g_i \neq 0$$

which is in contrast with the positive definiteness of V . Therefore, g_i cannot be nonzero. As i is chosen arbitrarily from $\{1, 2, \dots, d\}$, the derivative of V with respect to any of its arguments is zero at the origin, meaning that, $\nabla_{\mathbf{x}} V(\mathbf{x})|_{\mathbf{x}=\mathbf{0}} = 0$. \square

Each stage of the RoA estimation algorithm expands the level set of the estimated Lyapunov function to sample from the gap $\mathcal{G} = S_{\alpha c}(V) \setminus S_c(V)$ surrounding the current estimate of the RoA for a $\alpha > 1$. Both too small and too large gaps are harmful to the stability of the growing RoA estimation algorithm. A too small gap results in too few samples and prolongs the number of growth stages. Moreover, if the gap is too small, it is more likely that all initial states taken from the gap either converges to the equilibrium or diverges. Therefore, the dataset for the optimization problem (7) will be highly skewed that slows down the learning process even further. A too large gap is also harmful as it may advance far beyond the true RoA of the system and many sampled initial states can diverge to unknown and potentially dangerous regions of the state space. As a result, investigating the growth rate of the gap \mathcal{G} as a function of the properties of V is desirable to regularize or prevent harmful sampling behaviors. The following theorem sheds light on this matter.

Theorem 12. *Growth rate of level sets: Assume $V : \mathcal{X} \rightarrow \mathbb{R}$ is a positive definite Lipschitz continuous function on $\mathcal{X} \subseteq \mathbb{R}^d$. Let $S_c(V) = \{\mathbf{x} \in \mathcal{X} : V(\mathbf{x}) \leq c\}$ be the region enclosed by the level set $\partial S_c(V) = \{\mathbf{x} \in \mathcal{X} : V(\mathbf{x}) = c\}$ at the level value c . If $G \leq \|\nabla_{\mathbf{x}} V(\mathbf{x})\|$ for $G \in \mathbb{R}^{>0}$ and $\mathbf{x} \in S_c(V)$, then $\partial\mu(S_c(V)) \setminus \partial c \propto G^{-1}$.*

Proof. Let $\mathbf{z} = z \nabla_{\mathbf{x}} V(\mathbf{x}) / \|\nabla_{\mathbf{x}} V(\mathbf{x})\|$ be a tiny perturbation in the direction of the normal to the level set. V is expanded around $\mathbf{x} \in \partial S_c(V)$ as

$$\begin{aligned} V(\mathbf{x} + \mathbf{z}) &= V(\mathbf{x}) + \nabla_{\mathbf{x}} V(\mathbf{x})^T \mathbf{z} + O(z^2) \\ &= V(\mathbf{x}) + z \|\nabla_{\mathbf{x}} V(\mathbf{x})\| + O(z^2) \end{aligned}$$

where $O(z^2)$ can be ignored for sufficiently small $z = \|\mathbf{z}\|$. For $\alpha \in \mathbb{R}^{>1}$ and sufficiently close to 1,

$$\begin{aligned} S_{\alpha c}(V) &= \{\mathbf{x} + \mathbf{z} : \mathbf{x} \in \partial S_c(V) \text{ and } V(\mathbf{x}) + \nabla_{\mathbf{x}} V(\mathbf{x})^T \mathbf{z} \leq \alpha c\} \\ &= \{\mathbf{x} + \mathbf{z} : \mathbf{x} \in \partial S_c(V) \text{ and } z \|\nabla_{\mathbf{x}} V(\mathbf{x})\| \leq (\alpha - 1)c\}. \end{aligned}$$

As G is assumed to be a lower bound of $\|\nabla_{\mathbf{x}} V(\mathbf{x})\|$, $z \|\nabla_{\mathbf{x}} V(\mathbf{x})\| \leq (\alpha - 1)c$ implies $z \leq c(\alpha - 1) \|\nabla_{\mathbf{x}} V(\mathbf{x})\|^{-1} \leq c(\alpha - 1)G^{-1}$.

Notice that $\partial S_c(V)$ is a $(d - 1)$ -dimensional surface that encloses $S_c(V)$ an d -dimensional volume that are both embedded in a d -dimensional embedding space \mathcal{X} . We are interested in the volume of $\mathcal{G} := S_{\alpha c}(V) \setminus S_c(V)$. Assume $d\omega$ is the differential form for \mathcal{G} . We can write $d\omega = ds \|\mathbf{z}\| = z ds$ where ds is the surface differential form for $\partial S_c(V)$. Hence,

$$\mu(\mathcal{G}) = d\mu(S_c(V)) = \int_{\mathcal{G}} d\omega = \int_{\partial S_c(V)} z ds \leq c(\alpha - 1)G^{-1} \int_{\partial S_c(V)} ds. \quad (12)$$

where $\int_{\partial S_c(V)} ds$ does not depend on α or G . Hence, by pushing $\alpha \rightarrow 0$, $\partial\mu(S_c(V)) \setminus \partial c = c\mu(\partial S_c(V))G^{-1} \propto G^{-1}$ that completes the proof. \square

As a result of this theorem, in some applications, one may need to control $\|\nabla_{\mathbf{x}} V(\mathbf{x})\|$ for $\mathbf{x} \in \partial S_c(V)$ to prevent sampling from a too large or too small gap.

D Theoretical Motivation of $[V(\mathbf{x}) - V_{\pi_{n-1}}(f_{\pi}(\mathbf{x}))]^2$ in Equation (7)

In this section we discuss the theory behind the term $[V(\mathbf{x}) - V_{\pi_{n-1}}(f_{\pi}(\mathbf{x}))]^2$ in Equation (7) that we added to facilitate learning the RoA. The objective function for the RoA estimation phase is restated here:

$$\mathcal{L}(V) = \sum_{\mathbf{x} \in \mathbb{X}^{\text{IN}}} [V(\mathbf{x}) - \bar{c}] - \sum_{\mathbf{x} \in \mathbb{X}^{\text{OUT}}} [V(\mathbf{x}) - \bar{c}] + \lambda_{\text{RoA}} \sum_{\mathbf{x} \in \mathbb{X}^{\text{IN}}} \Delta V(\mathbf{x}) + \lambda_{\text{monot}} \sum_{\mathbf{x} \in \mathbb{X}^{\text{IN}}} [V(\mathbf{x}) - V_{\pi_{n-1}}(f_{\pi_{n-1}}(\mathbf{x}))]^2.$$

As mentioned in Section 4.2, the first two terms construct a classifier objective. The third term is added to conform with the conditions of Theorem 1 and Corollary 1. Here, we focus on the last term, i.e., $[V(\mathbf{x}) - V_{\pi_{n-1}}(f_{\pi}(\mathbf{x}))]^2$. The motivation behind adding this term comes from the constructive method proposed in [56].

The idea of the constructive methodology of [56] is to construct a sequence of functions V_0, V_1, \dots for the autonomous dynamical system $\dot{\mathbf{x}}(t) = f(\mathbf{x}(t))$ in order to use the level sets of the accumulating function of this sequence for estimating the RoA of the vector field f . The theory is developed for a class of functions more general than Lyapunov functions that are called energy-like functions. An energy-like function decreases over the trajectories of the system (see [54] for a precise definition). Given an energy-like function V_0 for the vector field f , the following sequence of functions is constructed

$$\begin{aligned} V_1(\mathbf{x}) &= V_0(\mathbf{x} + \epsilon_1 f(\mathbf{x})) \\ V_2(\mathbf{x}) &= V_1(\mathbf{x} + \epsilon_2 f(\mathbf{x})) \\ &\dots \\ V_n(\mathbf{x}) &= V_{n-1}(\mathbf{x} + \epsilon_n f(\mathbf{x})) \end{aligned} \tag{13}$$

where $d_i, i = 1, 2, \dots, n$ are positive numbers. Two facts about this sequence must be proved: **1)** All functions produced in this sequence are energy-like functions. **2)** For a fixed positive c , $S_c(V_i) \subset S_c(V_{i+1})$. The following two theorems guarantee these points.

Theorem 13 (Energy-like functions, lemma 4.2 in [56]). *Let $V : \mathbb{R}^d \rightarrow \mathbb{R}$ be an energy-like function for the nonlinear autonomous system $\dot{\mathbf{x}}(t) = f(\mathbf{x}(t))$ with the equilibrium point $\bar{\mathbf{x}} = \mathbf{0}$. Let \mathcal{D} be a compact set around $\bar{\mathbf{x}}$ that contains no other equilibrium points. Then, there exists an $\hat{\epsilon} > 0$ such that for $\epsilon < \hat{\epsilon}$, the function $V_1 = V(\mathbf{x} + \epsilon f(\mathbf{x}))$ is also an energy-like function on the compact set \mathcal{D} for the vector field f .*

This theorem guarantees that all functions in the constructive process (13) are energy-like functions.

Theorem 14 (Monotonic level sets, lemma 4.1 in [56]). *Let $V : \mathbb{R}^d \rightarrow \mathbb{R}$ be an energy-like function for the nonlinear autonomous system $\dot{\mathbf{x}}(t) = f(\mathbf{x}(t))$ with the equilibrium point $\bar{\mathbf{x}} = \mathbf{0}$. Let \mathcal{D} be a compact set around $\bar{\mathbf{x}}$ that contains no other equilibrium points. Assume the set $S_c(V) := \{\mathbf{x} : V(\mathbf{x}) \leq c \text{ and } \mathbf{x} \in \mathcal{D}\}$ is non-empty for some constant c . Then there exists an $\tilde{\epsilon} > 0$ such that for the set characterized by $S_c(V_1) := \{\mathbf{x} : V_1(\mathbf{x}) \leq c \text{ and } \mathbf{x} \in \mathcal{D}\}$ where $V_1(\mathbf{x}) = V(\mathbf{x} + \epsilon f(\mathbf{x}))$ and $\epsilon < \tilde{\epsilon}$, the following holds*

$$S_c(V) \subset S_c(V_1). \tag{14}$$

This theorem guarantees that the sequence built by the constructive process (13) gives a monotonically increasing sequence of level sets. Therefore, this theorem, contributes to the satisfaction of Assumption 3.

Now, we get back to the added term to the objective function, i.e., $[V(\mathbf{x}) - V_{\pi_{n-1}}(f_{\pi_{n-1}}(\mathbf{x}))]^2$. Notice that $V_{\pi_{n-1}}(\cdot)$ is fixed and the minimization is performed with respect to $V(\cdot)$. In the realm of discrete systems, $\mathbf{x} + \epsilon f(\mathbf{x})$ is replaced by $f(\mathbf{x})$. Hence, minimizing the above term at each stage of the algorithm emulates the above constructive process.

E Algorithms

The proposed algorithms in this work are verbally described in Section 4. To facilitate implementation, the detailed pseudo-code of the algorithms come here. The RoA estimation phase is realized as Algorithm 1 and the policy update phase is realized as Algorithm 2.

F Model-Based Assumption

The model of the system is used to produce the trajectories of the system which is needed in evaluating both objective functions in (8) and (7). In the following, we show that the knowledge of the model of the system can be relaxed in both phases of the algorithm.

F.1 RoA Estimation Phase

As can be seen in Equation (7) and Algorithm 1, in this phase, the model is used to produce trajectories starting from the sampled initial states from the gap around the current estimate of the RoA or from within the RoA. In both cases, as also suggested by [55], the real system can be used to produce

Algorithm 1: RoA estimation: $(\mathcal{R}_{\pi_{n-1}}, \pi_n) \rightarrow \mathcal{R}_{\pi_n}$

input : $(V_{\pi_{n-1}}, c_{n-1})$: The Lyapunov function and level value of stage n where $\mathcal{R}_{\pi_{n-1}} = \mathcal{S}_{c_{n-1}}(V_{\pi_{n-1}}) \mid f_{\pi_{n-1}}$: Closed-loop system vector field $\mid \gamma_r > 1$: Level value multiplicative factor $\mid N \in \mathbb{N}$: Number of sampled states $\mid M \in \mathbb{N}$: Number of stages $\mid 0 \leq \beta_r \leq 1$: Mixture parameter $\mid L_r \in \mathbb{N}$: Trajectory length $\mid \mathcal{D}$: Domain $\mid \lambda_{\text{RoA}}$: Negative definiteness weighting factor $\mid \lambda_{\text{monot}}$: Monotonicity weighting factor

output : (V_{π_n}, c_n)

- 1 Init \hat{V} to $V_{\pi_{n-1}}$ and \hat{c} to c_{n-1}
- 2 Init the sampling distribution p_r to $U(\mathcal{D})$, i.e., uniform distribution over the domain \mathcal{D}
- 3 **for** $m = 1, \dots, M$ **do**
- 4 $\mathcal{G} \leftarrow \mathcal{S}_{\gamma_r \hat{c}}(\hat{V}) \setminus \mathcal{S}_{\hat{c}}(\hat{V})$
- 5 $p_r \leftarrow \beta_r U(\mathcal{G}) + (1 - \beta_r) U(\mathcal{D})$
- 6 $\mathbb{X}_0 \leftarrow$ Generate N samples from p_r
- 7 $\mathbb{X}_{L_r} \leftarrow$ Run $f_{\pi_{n-1}}$ on \mathbb{X}_0 for L_r steps
- 8 $\mathbb{X}_0^{\text{IN}} \leftarrow \{(\mathbf{x}, 1) : \mathbf{x} \in \mathbb{X}_0, \Phi(\mathbf{x}, L_r) \in \mathcal{S}_{\hat{c}}(\hat{V})\}$
- 9 $\mathbb{X}_0^{\text{OUT}} \leftarrow \{(\mathbf{x}, 0) : \mathbf{x} \in \mathbb{X}_0, \Phi(\mathbf{x}, L_r) \notin \mathcal{S}_{\hat{c}}(\hat{V})\}$
- 10 $V^* \leftarrow$ Optimize for V in the objective function (7) using the dataset $\{\mathbb{X}_0^{\text{IN}}, \mathbb{X}_0^{\text{OUT}}\}$
- 11 $\hat{c} \leftarrow \text{argmax}_c \{c \in \mathbb{R} : \Delta f_{\pi_{n-1}}(\mathbf{x}) < 0 \text{ for } \mathbf{x} \in \mathcal{S}_c(V^*)\}$
- 12 $\hat{V} \leftarrow V^*$
- 13 **end**
- 14 $(V_{\pi_n}, c_n) \leftarrow (\hat{V}, \hat{c})$

Algorithm 2: Policy update: $\mathcal{R}_{\pi_n} \rightarrow \pi_{n+1}$

input : (V_{π_n}, c_n) : The Lyapunov function and level value of stage n where $\mathcal{R}_{\pi_n} = \mathcal{S}_{c_n}(V_{\pi_n}) \mid$ Closed-loop system vector field $f_{\pi_n} \mid \gamma_p > 1$: Level value multiplicative factor $\mid N \in \mathbb{N}$: Number of sampled states $\mid 0 \leq \beta_p \leq 1$: Mixture parameter $\mid L_p \in \mathbb{N}$: Trajectory length $\mid \lambda_u$: Unstable states weighting factor

output : π_{n+1}

- 1 Init sampling distribution p_p to $U(\mathcal{S}_{c_n}(V_{\pi_n}))$, i.e., uniform distribution over $\mathcal{S}_{c_n}(V_{\pi_n})$
- 2 $\mathcal{G} \leftarrow \mathcal{S}_{\gamma_p c_n}(V_{\pi_n}) \setminus \mathcal{S}_{c_n}(V_{\pi_n})$
- 3 $p_p \leftarrow \beta_p U(\mathcal{G}) + (1 - \beta_p) U(\mathcal{S}_{c_n}(V_{\pi_n}))$
- 4 $\mathbb{X}_0 \leftarrow$ Generate N samples from p_p
- 5 $\pi_{n+1} \leftarrow$ Optimize for π in the objective function (8) using the dataset $\{\mathbb{X}_0\}$

the trajectories rather than the model. Assuming that γ_r is small enough in Algorithm 1 and with the considerations that we proved in Theorem 12, the gap from which the initial states are sampled is not too large. Hence, in an approach similar to active learning, the real system can be used to produce the trajectories and label them based on whether they enter the current target level set of the estimated Lyapunov function or not. Hence, in this phase, there will be no need to know the model of the system or estimate it.

F.2 Policy Update Phase

The model requirement is a bit different in this phase compared with the RoA estimation phase. As we need to update the policy, the way the behavior of the system changes with respect to a change in the policy is required. However, looking at (8), it is observed that the behavior of the system influences the objective function only via the Lyapunov function $V(\Phi(\mathbf{x}, L_p))$. Suppose the policy is parameterized as $\pi(\mathbf{x}; \phi)$. Then, the closed-loop system becomes $\mathbf{x}_{k+1} = f(\mathbf{x}_k, \pi(\mathbf{x}_k))$. The required gradient to update the policy parameters contains $\partial V(\mathbf{x}_k) / \partial \psi$ where the information of ψ is encoded in $\mathbf{x}_k = \Phi(\mathbf{x}_0, k)$. The derivative decomposes as

$$\frac{\partial V(\mathbf{x}_k)}{\partial \psi} = \frac{\partial V(\mathbf{x}_k)}{\partial \mathbf{x}_k} \frac{\partial \mathbf{x}_k}{\partial \psi} \quad (15)$$

where the knowledge of the model is required to compute $\partial \mathbf{x}_k / \partial \psi$ that will be a matrix of size $\dim(\mathcal{X}) \times \dim(\psi)$. When the model is not given, one must instead try to estimate the model of the system $\hat{f} : \mathbb{R}^d \rightarrow \mathbb{R}^d$. However, this vector-valued function is difficult to estimate unless in very limited cases. Instead, one can try to directly estimate V rather than f as a function of ψ . As V is a scalar-valued function, it takes fewer trajectories to give a good estimate of $\partial V / \partial \psi$. Hence, even though the model of the system is needed for this phase, there are two factors that relaxes this requirement: **1)** As the trajectories are integrated forward only for L_p steps in Algorithm 2, a local estimation would be sufficient. **2)** Even in the local estimate, one does not need to estimate the nonlinear vector field as an \mathbb{R}^d to \mathbb{R}^d function. What matters is how the vector field looks like through the lens of the Lyapunov function that is a scalar-valued function. Hence, an $\mathbb{R}^d \rightarrow \mathbb{R}^d$ estimation problem can be replaced by an $\mathbb{R}^d \rightarrow \mathbb{R}$ estimation problem.

G Weak Learning Signal

In this section, we take a closer look at the occasions that the learning signal for the policy update stage of the algorithm (see Section 4.3) is weak. We discuss the problem for a general setting and show that the setting of this paper is a special case.

Problem Statement. Assume the discrete-time time-invariant non-autonomous dynamical system $\mathbf{x}_{k+1} = f(\mathbf{x}_k, \mathbf{u}_k)$. The goal is to design \mathbf{u}_k for $0 \leq k \leq T$ such that \mathbf{x}_k meets some specified conditions. In the Lyapunov stability analysis, these conditions are assessed by a function $V : \mathcal{X} \rightarrow \mathbb{R}^{\geq 0}$, i.e., after rolling out the starting state \mathbf{x}_0 for T steps by the dynamics f controlled by \mathbf{u}_k , $V(\mathbf{x}_{-T}) \in \mathcal{S}$ where \mathcal{S} encapsulates the desired conditions for the trajectory $\mathbf{x}_{-T} = (\mathbf{x}_0, \mathbf{x}_1, \dots, \mathbf{x}_T)$ of the system. Assume the deviation of $V(\mathbf{x}_{-T})$ from its desired set \mathcal{S} is measured by a deviation metric $\mathcal{L}(V(\mathbf{x}_{-T}), \mathcal{S})$. In many control tasks such as *tracking*, the entire trajectory matters, and \mathcal{L} will be a function of every state in the trajectory. However, in control tasks such as *reaching*, only the final state \mathbf{x}_T matters; consequently the objective function \mathcal{L} only depends on \mathbf{x}_T . Stability, in the presence of a Lyapunov function, can be seen as an example of the second class of tasks where the relative position of \mathbf{x}_T compared to the level sets of the Lyapunov function is sufficient to decide the convergence of that trajectory. In practice, the control signal \mathbf{u}_k is produced as a parametric function of states $\mathbf{u}_k = \pi(\mathbf{x}_k; \psi)$. Therefore, the entire trajectory $\mathbf{x}_{-T}(\psi)$ is now parameterised by ψ and so is the loss function $\mathcal{L}(\psi)$. The class of algorithms known as *policy gradient* uses $\partial \mathcal{L}(\psi) / \partial \psi$ to learn the controller $\pi(\cdot; \psi)$. In this section, we study the condition of this gradient and show under which circumstances it vanishes and results in slow convergence.

In a general case where V in $\mathcal{L}(V(\mathbf{x}_{-T}), \mathcal{S})$ is a function of the entire trajectory \mathbf{x}_{-T} , the gradient w.r.t. the controller parameters is written as:

$$\frac{\partial \mathcal{L}}{\partial \psi} = \sum_{1 \leq p \leq T} \frac{\partial \mathcal{L}_p}{\partial \psi} \quad (16)$$

$$\frac{\partial \mathcal{L}_k}{\partial \psi} = \sum_{1 \leq p \leq k} \left(\frac{\partial \mathcal{L}}{\partial \mathbf{x}_k} \frac{\partial \mathbf{x}_k}{\partial \mathbf{x}_p} \frac{\partial^+ \mathbf{x}_k}{\partial \psi} \right) \quad (17)$$

$$\frac{\partial \mathbf{x}_k}{\partial \mathbf{x}_p} = \prod_{p < i \leq k} \frac{\partial \mathbf{x}_i}{\partial \mathbf{x}_{i-1}} = \prod_{p < i \leq k} \left(\frac{\partial f}{\partial \mathbf{x}} \Big|_{\mathbf{x}=\mathbf{x}_{i-1}} + \frac{\partial f}{\partial \mathbf{u}} \Big|_{\mathbf{u}=\pi(\mathbf{x}_{i-1})} \frac{\partial \pi(\mathbf{x})}{\partial \mathbf{x}} \Big|_{\mathbf{x}=\mathbf{x}_{i-1}} \right) \quad (18)$$

The gradients are derived as sum-of-products and $\frac{\partial^+ \mathbf{x}_k}{\partial \psi}$ refers to the *immediate* partial derivative of state \mathbf{x}_k with respect to ψ when \mathbf{x}_{k-1} is considered as a constant.

In the special case where V is the Lyapunov function in $\mathcal{L}(V(\mathbf{x}_{-T}), \mathcal{S})$ and the concern is the stability of the system, $V(\mathbf{x}_{-T}) = V(\mathbf{x}_T)$, meaning that the sum on the r.h.s of (16) will only have one term $\partial \mathcal{L}_T / \partial \psi$ and (17) will transform to

$$\frac{\partial \mathcal{L}_T}{\partial \psi} = \frac{\partial \mathcal{L}}{\partial \mathbf{x}_T} \sum_{1 \leq k \leq T} \left(\frac{\partial \mathbf{x}_T}{\partial \mathbf{x}_k} \frac{\partial^+ \mathbf{x}_k}{\partial \psi} \right). \quad (19)$$

In the following, we analyze the role of each term that contributes to this gradient.

G.1 The Component $\frac{\partial \mathcal{L}}{\partial \mathbf{x}_T}$

This term concerns the differential condition of $\mathcal{L}(\mathbf{x}) = \mathcal{L}(V(\mathbf{x}), \mathcal{S})$ at $\mathbf{x} = \mathbf{x}_T$ as

$$\frac{\partial \mathcal{L}(\mathbf{x})}{\partial \mathbf{x}} \Big|_{\mathbf{x}=\mathbf{x}_T} = \frac{\partial \mathcal{L}(V)}{\partial V} \Big|_{V=V(\mathbf{x}_T)} \frac{\partial V(\mathbf{x})}{\partial \mathbf{x}} \Big|_{\mathbf{x}=\mathbf{x}_T} \quad (20)$$

If any of these terms gets too small, the overall gradient gets small too resulting in a vanishing gradient issue. To avoid this, the algorithm must ensure that these terms remain sufficiently large. For the first term $\partial \mathcal{L}(V)/\partial V$, this condition is normally fulfilled if the deviation metric $\mathcal{L}(\cdot, \cdot)$ is designed properly. For example, one candidate function for \mathcal{L} would be a signed distance function that measures how far \mathbf{x}_T is from the maximal stable level set $\partial S_{c_{\max}}(V)$, e.g., $\mathcal{L}(V(\mathbf{x}_T), S_{c_{\max}}(V)) = V(\mathbf{x}_T) - c_{\max}$. Another candidate deviation metric could be $\mathcal{L}(V(\mathbf{x}_T), S_{c_{\max}}(V)) = \max((V(\mathbf{x}_T) - c_{\max}), 0)$ that does not care about the actual value of $V(\mathbf{x}_T)$ as long as \mathbf{x}_T lives within the level set $S_{c_{\max}}(V)$. For the former case, $\partial \mathcal{L}/\partial V = V$ meaning that the gradient does not vanish as long as $\mathbf{x}_T \neq \bar{\mathbf{x}}$.

The second term of the r.h.s of (20) depends on the slope of the function V evaluated at the final state of the trajectory. If V is a candidate Lyapunov function, $\nabla_{\mathbf{x}} V(\mathbf{x})$ vanishes at the equilibrium as we proved in Lemma 11. Therefore, if \mathbf{x}_T is too close to the equilibrium (i.e., the system converges), the learning signal to update the policy will vanish. This point is formalized in the following remark.

Remark 15. Consider the closed-loop system $\dot{\mathbf{x}} = f(\mathbf{x}, \pi(\mathbf{x}))$. Let \mathbf{x}_0 be the initial state of a trajectory that starts from within the RoA of the equilibrium point $\bar{\mathbf{x}}$ of the closed-loop system denoted by $\mathcal{R}_{\pi}^{\bar{\mathbf{x}}}$. Let V be the Lyapunov function and the objective function $\mathcal{L}(V_{\pi}(\mathbf{x}_T), \mathcal{S})$ is optimized to update the policy π . One must be careful not to let the trajectories roll out for too long ($T \gg 1$). As \mathbf{x}_T gets too close to the equilibrium, the information of the trajectory degenerates (see Theorem 16) and the gradient to update the controller vanishes (see Lemma 11). On the other hand, if \mathbf{x}_0 does not belong to the RoA of $\bar{\mathbf{x}}$, it can go too far from $\mathcal{R}_{\pi}^{\bar{\mathbf{x}}}$ and may escape the validity domain of the Lyapunov function V . Hence, in either case, the length T of the trajectory influences the information content of the trajectory for updating the policy. Both too large and too small values of T must be avoided when the trajectories pass through the Lyapunov function. Too small values of T are non-informative due to the continuity of V . Too large values of T , on the other hand, is non-informative as the trajectory enters the flat regions of V or escape the domain of validity of V .

Theorem 16. Consider the dynamical system $\dot{\mathbf{x}}(t) = f(\mathbf{x}(t), \mathbf{u}(t))$ where the control signal is issued by the policy function $\mathbf{u}(t) = \pi(\mathbf{x}(t); \psi)$ that is parameterised by ψ . Let $\bar{\mathbf{x}} = \mathbf{0}$ be an asymptotic equilibrium point of this system. If $\mathbf{x}(0) \in \mathcal{R}_{\pi}^{\mathbf{0}}$ and $V : \mathcal{X} \rightarrow \mathbb{R}^{0 \geq}$ is a C^r Lyapunov function with $r \geq 1$, then

$$\forall \epsilon > 0, \exists T > 0 \text{ such that } \left\| \frac{\partial V(\mathbf{x})}{\partial \psi} \Big|_{\mathbf{x}=\mathbf{x}_T} \right\| < \epsilon \quad (21)$$

Proof. It can be seen in (19) that $\nabla_{\mathbf{x}} V$ appears multiplicatively in $\nabla_{\psi} V$. As stated in Lemma 11, $\nabla_{\mathbf{x}} V(\mathbf{x}) = 0$ at $\bar{\mathbf{x}} = \mathbf{0}$ that makes $\nabla_{\psi} V$ vanish as well at the equilibrium point. Now suppose $V \in C^r (r \geq 1)$ with respect to both its arguments \mathbf{x} and \mathbf{u} . Moreover, $\pi(\cdot, \psi)$ is assumed to be smooth with respect to its parameters ψ . Therefore, the map $\psi \rightarrow \nabla_{\psi} V$ is continuous. Furthermore, $\mathbf{x}(t) \rightarrow \mathbf{0}$ as $t \rightarrow \infty$ because $\mathbf{x}(0) \in \mathcal{R}_{\pi}^{\mathbf{0}}$. The continuity of the map $\psi \rightarrow \nabla_{\psi} V$ together with the above result on vanishing $\nabla_{\psi} V$ at the equilibrium point completes the proof. \square

G.2 The Component $\frac{\partial \mathbf{x}_k}{\partial \mathbf{x}_p}$

This term determines how state information propagates forward through the trajectory. More precisely, it shows how perturbing a state at time p affects the downstream state \mathbf{x}_k after $k - p$ time steps when the parameters of the system are kept fixed. In the following, we take a closer look at constituent terms of (18). We first define the function

$$J_i(\mathbf{x}_i, \mathbf{u}_i) = \left[\frac{\partial f}{\partial \mathbf{x}} \Big|_{\mathbf{x}=\mathbf{x}_i}, \frac{\partial f}{\partial \mathbf{u}} \Big|_{\mathbf{u}=\mathbf{u}_i} \right]^{\top} \quad (22)$$

that is different from (18) in the sense that \mathbf{u}_i is not necessarily a function of \mathbf{x}_i . Due to the fact that $\partial \mathbf{x}_k / \partial \mathbf{x}_p$ equals the product of $J_i = J_i(\mathbf{x}_i, \mathbf{u}_i)$ along the trajectory $\{(\mathbf{x}_i, \mathbf{u}_i)\}_{i=1}^{k-1}$, a measure of the size of J_i would be informative about the influence of \mathbf{x}_p on \mathbf{x}_k . First, we consider the vanishing

gradient issue when the influence becomes too small. Notice that the size of J_i as defined in (22) is determined by two terms as (we drop the index i for convenience)

$$\|J(\mathbf{x}, \mathbf{u})\| \leq \left\| \frac{\partial f}{\partial \mathbf{x}} \right\| + \left\| \frac{\partial f}{\partial \mathbf{u}} \right\| \quad (23)$$

If the closed-loop dynamics f_π is Lipschitz continuous (as it is assumed in Section 2 to ensure the existence and uniqueness of the solution), both terms on the r.h.s. of the inequality (23) will be bounded. However, the condition of Equation (22) is a more general case when \mathbf{u} is not necessarily a function of the states. In this case, f must be Lipschitz in both \mathbf{x} and \mathbf{u} , that is, there exists positive constants L_{f_x} and L_{f_u} such that:

$$\|\partial f(\mathbf{x}, \mathbf{u})/\partial \mathbf{x}\| \leq L_{f_x}, \quad \forall \mathbf{u} \in \mathcal{U} \text{ and } \forall \mathbf{x} \in \mathcal{X} \quad (24)$$

$$\|\partial f(\mathbf{x}, \mathbf{u})/\partial \mathbf{u}\| \leq L_{f_u}, \quad \forall \mathbf{u} \in \mathcal{U} \text{ and } \forall \mathbf{x} \in \mathcal{X}. \quad (25)$$

Intuitively, this means that the open-loop dynamics $f(\mathbf{x}, \mathbf{u})$ rolls out smoothly and does not respond too harshly to the changes in the control input. If a component of the system breaks down under some control input, $\mathbf{u} \in \mathcal{U}$, the above conditions do not hold. In addition, it might be the case that the dynamics of the system show high-frequency vibrations under some specific control inputs (e.g. when the controller excites the natural frequency of the system). These conditions occur rarely in physical systems when the controller remain within a reasonable range but may happen frequently under *adversarial* regimes when the system is intentionally attacked by an unauthorized user. Such regimes are beyond the scope of this paper. Hence, we can reasonably assume that J_i is upper bounded by $2 \times \max(L_{f_{x_i}}, L_{f_{u_i}})$.

A more general control signal consists of two parts. The first part is a function of states and the second part is open-loop. Therefore, we have:

$$\mathbf{u}_i = \pi(\mathbf{x}_i; \psi) + \tilde{\mathbf{u}}_i \text{ with } \frac{\partial \tilde{\mathbf{u}}_i}{\partial \mathbf{x}_i} = 0.$$

We can write the overall dynamics as $\mathbf{x}_{i+1} = f(\mathbf{x}_i, \mathbf{u}_i) = f(\mathbf{x}_i, (\pi(\mathbf{x}_i), \tilde{\mathbf{u}}_i)) = f(\mathbf{x}_i, \tilde{\mathbf{u}}_i)$ which transforms to the case of (22) with the difference that the policy function $\pi(\mathbf{x})$ is now absorbed in the first component of (22). Hence, $J_i(\mathbf{x}_i, \tilde{\mathbf{u}}_i)$ decomposes as

$$J_i(\mathbf{x}_i, \tilde{\mathbf{u}}_i) = \left[\frac{\partial f}{\partial \mathbf{x}} \Big|_{\mathbf{x}=\mathbf{x}_i} + \frac{\partial f}{\partial \pi(\mathbf{x})} \Big|_{\pi(\mathbf{x})=\pi(\mathbf{x}_i)}, \frac{\partial f}{\partial \tilde{\mathbf{u}}} \Big|_{\tilde{\mathbf{u}}=\tilde{\mathbf{u}}_i} \right]^\top$$

Observe that Equation (18) depends only on the first block of $J_i(\mathbf{x}_i, \tilde{\mathbf{u}}_i)$ and $\partial f/\partial \tilde{\mathbf{u}}$ does not affect the gradient even though it affects the trajectory that the system passes. As a result, the influence of the open-loop control signal $\tilde{\mathbf{u}}_t$ on $\partial \mathcal{L}/\partial \psi$ is via the final states of the trajectory \mathbf{x}_T as well as $\partial \mathcal{L}/\partial \mathbf{x}_T$ in (19).

H Training Details

H.1 Lyapunov Function

A parametric candidate Lyapunov function $V(\cdot; \theta)$ must satisfies the conditions of (4). It must be positive definite on a domain \mathcal{D} and its value must decrease along the trajectories of the system. As the second condition depends on the system, it is embedded in the optimization loss function (7). The first condition (positive definiteness) though does not depend on the system. It must be enforced for every $\mathbf{x} \in \mathcal{D}$. Rather than including it in the loss function, we restrict the hypothesis set $V(\cdot; \theta) \in \mathcal{H}$ to the class of positive definite functions. In kernel methods, this property can be achieved by a proper choice of kernels. With neural networks, $V(\cdot; \theta)$ can be parameterized by $V(\mathbf{x}; \theta) = v(\mathbf{x}; \theta)^\top v(\mathbf{x}; \theta)$ as a Lyapunov candidate function where $v(\mathbf{x}; \theta)$ is a multilayer perceptron. This guarantees the non-negativeness of $V(\cdot; \theta)$. To ensure $V(\mathbf{x}; \theta)$ does not vanish at any point other than the origin, first suppose \mathbf{z}_ℓ and $\mathbf{z}_{\ell+1}$ are the input and output of the ℓ^{th} layer respectively, i.e., $\mathbf{z}_{\ell+1} = \zeta_\ell(W\mathbf{z}_\ell)$ where W is the weight matrix and $\zeta_\ell(\cdot)$ is the activation matrix. To guarantee the strict positiveness of $v(\mathbf{x}; \theta)$ for $\mathbf{x} \neq \mathbf{0}$, both activation matrix ζ_ℓ and weight matrix $W_\ell \in \mathbb{R}^{d_\ell \times d_{\ell+1}}$ must have trivial nullspaces. Activation functions such as tanh and ReLU meet this condition. The weight matrix can be constructed as the following:

$$\mathbf{W}_\ell = \begin{bmatrix} \mathbf{G}_{\ell 1}^\top \mathbf{G}_{\ell 1} + \varepsilon \mathbf{I}_{d_{\ell-1}} \\ \mathbf{G}_{\ell 2} \end{bmatrix} \quad (26)$$

where $\mathbf{G}_{\ell 1} \in \mathbb{R}^{q_\ell \times d_{\ell-1}}$ for some $q_\ell \in \mathbb{N}_{\geq 1}$, $\mathbf{G}_{\ell 2} \in \mathbb{R}^{(d_\ell - d_{\ell-1}) \times d_{\ell-1}}$, $\mathbf{I}_{d_{\ell-1}} \in \mathbb{R}^{d_{\ell-1} \times d_{\ell-1}}$ is the identity matrix and $\epsilon \in \mathbb{R}_+$ is a positive constant to ensure the upper block has full rank. See Remark 1 in the appendix of [55].

In our experiments, $v(\mathbf{x}; \theta)$ is represented by a 3-layer multilayer perceptron each layer of dimension 64 followed by tanh activation functions and a linear last layer.

I Discretized Time and State Space

We discretize the dynamics of the inverted pendulum with time resolution of $\Delta T = 0.01$. The state space is also discretized in the rectangle $[\theta_{\min}, \theta_{\max}] = [-\pi/2, \pi/2]$, $[\omega_{\min}, \omega_{\max}] = [-2\pi, 2\pi]$. Each dimension is divided equally into 100 sections to form a 2-dimensional grid. Therefore, all the computations of Section 5 takes place with a finite set of states. For example, the true RoA denoted by the green plot in Figure 5 is computed by integrating forward all states of the state space grid. If the resolution of the grid is too coarse, the bound on the negative definiteness of $\Delta V(\mathbf{x})$ must change from 0 to a more conservative negative value in order to make sure the critical conditions of Equation (4) and Corollary 1 will not be violated. The new bound depends on the Lipschitz constants of V and f (see [55] for the detailed derivation of the bound).

J Hyper-parameters

The pre-training phase is performed with the learning rate 0.001 and $10k$ training steps. Each run of the RoA estimation algorithm is performed with the learning rate 0.01 and $10k$ training steps. Each run of the policy update phase is performed with the learning rate 0.01 with 100 steps. The number of learning steps in the policy update phase is a proxy to the distance between the current policy and the updated policy. Hence, by keeping this number fairly small, we make sure the condition of Assumption 2 is likely to be fulfilled.

In Equation (7), λ_{RoA} is set to 1000 to enforce the critical negative definiteness condition of Theorem 1 and Corollary 1. In the same equation, λ_{monot} is set to 0.01 to encourage to monotonicity of the RoA estimation algorithm. In Equation (8), λ_u is set to 10 to put more emphasis on stabilizing the unstable states compared with keeping stable the already stable states.

The sampling mixture parameters β_r and β_p are both set to 0.6 in Algorithms 1 and 2 respectively.

The length of the integrated trajectories (L_r, L_p) is set to 10 for both RoA estimation (see Algorithm 1) and policy update (see Algorithm 2) phases.

The multiplication constants γ_r and γ_p for both RoA estimation and policy update phases is set to 4.

The number of RoA estimation stages m in Algorithm 1 is set to 20. The total number of policy update phases is also set to 20. One can alternatively use a context-aware stopping criterion. For instance, updating the policy can be stopped when no significant change in the RoA or the policy parameters is observed.

The number of sampled initial states N is initialized to 10 in Algorithms 1 and 2 and increases by 10 after each update of the policy. The heuristic reason is that after each policy update, the RoA enlarges and it takes more samples to obtain a good representative of the gap surrounding the RoA.

K More Experimental Results

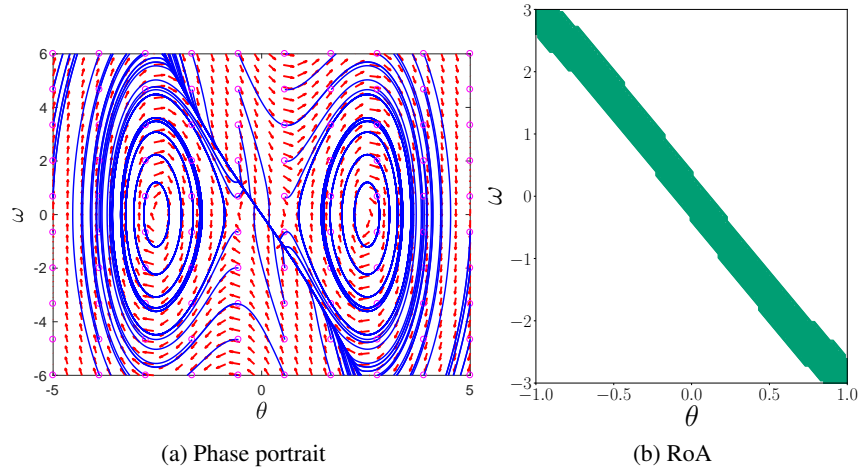


Figure 6: Dynamics of the inverted pendulum and its initial RoA for an LQR controller

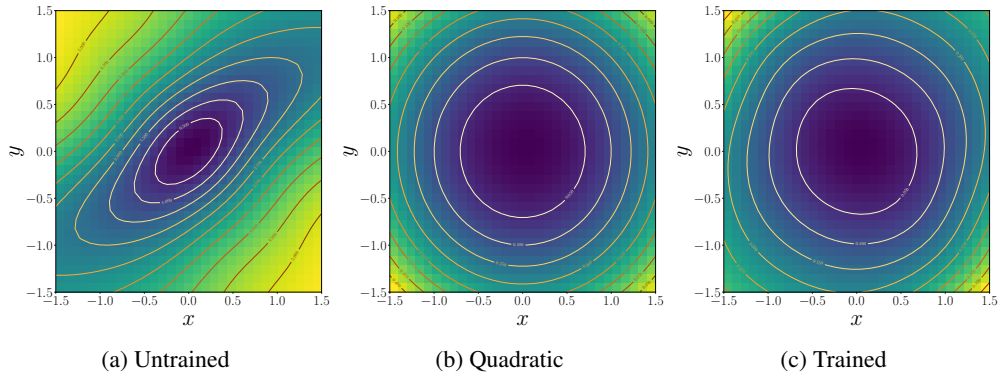


Figure 7: Pre-training the neural network with a quadratic Lyapunov function. The background heatmap represents the value of the underlying function. Lighter regions correspond to larger values. (a) The level sets of the untrained initialized neural network. (b) The target quadratic function (2) The level sets of the neural network pre-trained with the quadratic function of Figure 7b.

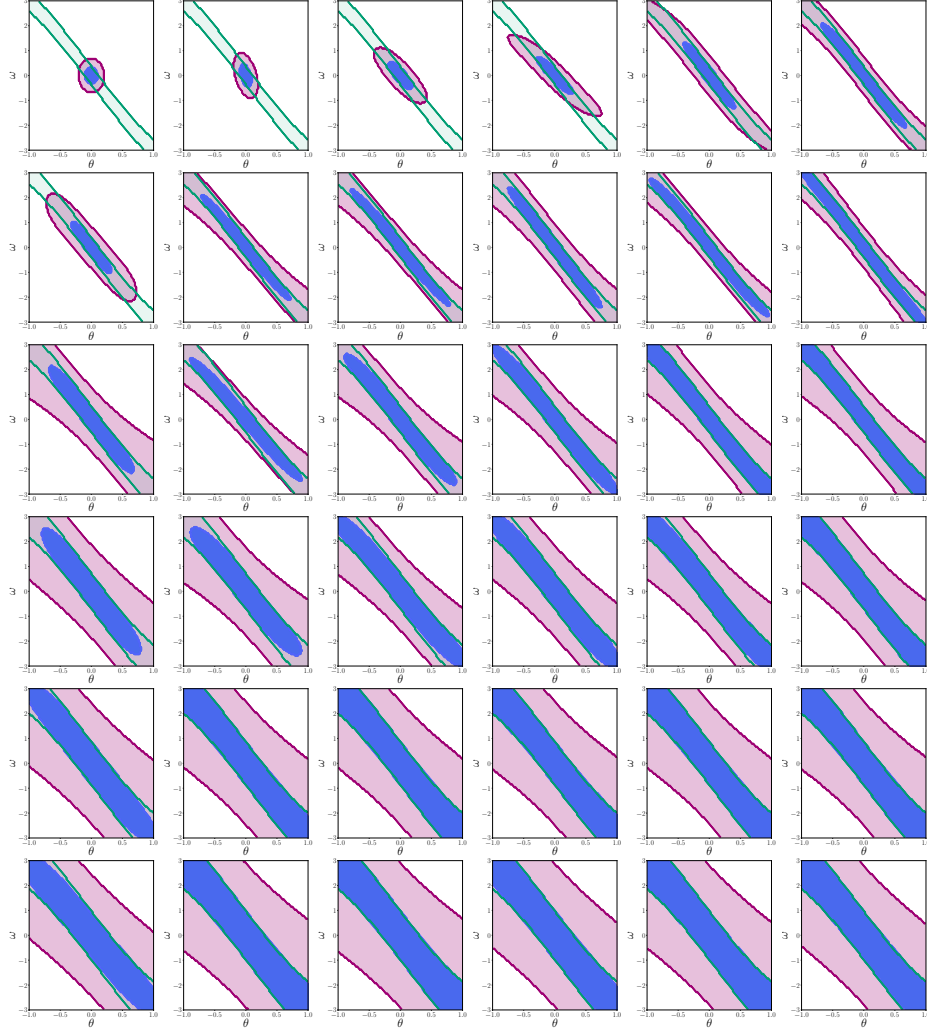


Figure 8: Visualizing the true RoA which is enlarged by the improved policy and is chased by a learned Lyapunov function. Each row corresponds to a policy update stage and each column corresponds to a RoA estimation stage. At each row, from left to right, the policy is fixed that results in a fixed true RoA (green plot). The columns from left to right are the stages of the RoA estimation phase (see Algorithm 1). The blue color is the estimated RoA $S_{c_n}(V_{\pi_n})$ and the pink color shows the gap $\mathcal{G} = S_{\gamma_{c_n}}(V_{\pi_n}) \setminus S_{c_n}(V_{\pi_n})$ that is used in Algorithms 1 and 2 for sampling the initial states. After the RoA estimation phase is done (the rightmost figure of each row), the policy update phase is performed. The leftmost figure in the next row shows that the true RoA enlarges as a result of the policy update. The RoA estimation phase continues from its latest stage which is a decent initial approximate for the enlarged RoA. As a result of the alternate application of RoA estimation and policy update phases, the bottom rightmost figure shows a significantly larger RoA compared with the top leftmost figure (see the green boundary of the true RoA around the blue region that is the estimated RoA by the learned Lyapunov function). Note that the Lyapunov function is also learned such that its level set (blue region) almost perfectly matches the true RoA (green boundary) in the bottom rightmost figure.